

# Supporting information of Insights into the Roles of Water on the Aqueous Phase Reforming of Glycerol

Tianjun Xie, Cameron J. Bodenschatz, and Rachel B. Getman \*

Chemical and Biomolecular Engineering Department, Clemson University

December 7, 2018

---

\*rgetman@clemson.edu

# 1 VASP INCAR settings

## 1.1 Geometry Optimization

The following INCAR parameters are intended for geometry optimization runs in VASP, for a system consists of Pt, C, O, and H atoms.

NWRITE = 1

LWAVE = .FALSE. ! write WAVECAR?

LCHARG = .FALSE. ! write CHGCAR?

LVTOT = .FALSE. ! write LOCPOT?

Electronic relaxation

IALGO = 48 ! 8: CG, 48: DIIS algorithm for electrons

ENCUT = 400

ALGO = Fast

ISMEAR = 0 ! 0: Gaussian, electron smearing

SIGMA = 0.100

PREC = accurate

LREAL = Auto

ROPT = 2e-4 2e-4 2e-4 2e-4

ISTART = 0

ADDGRID = T

NELM = 1000

NELMIN = 6

EDIFF = 1e-6

ISPIN = 1 ! polarization?

Ionic relaxation

NSW = 150 ! # of steps in optimization (default 0!)

ISIF = 2 ! 0: relax ions, 1,2:relax ions,calc stresses, 3:relax ion+cell

IBRION = 1 ! 1: quasi-NR, 2:CG algorithm for ions

NFREE = 10 ! number of DIIS vectors to save

POTIM = 0.35 ! reduce trial step in optimization

EDIFFG = -0.03

Dispersion

LVDW = .TRUE.

VDW\_C6 = 42.440 1.750 0.700 0.140

VDW\_R0 = 1.750 1.452 1.342 1.001

DOS

RWIGS = 1.300 0.770 0.730 0.320 ! Wigner-Seitz radii

## 1.2 Nudged Elastic Band Simulations

The following INCAR parameters are intended for Climbing Image Nudged Elastic Band (CI-NEB) method in VASP, for a system consists of Pt, C, O, and H atoms.

NWRITE = 1

LWAVE = .FALSE. ! write WAVECAR?

LCHARG = .FALSE. ! write CHGCAR?

```

LVTOT = .FALSE. ! write LOCPOT?
Electronic relaxation
ENCUT = 400
ALGO = Fast
ISMEAR = 0 ! 0: Gaussian, electron smearing
SIGMA = 0.100
PREC = med
LREAL = Auto
LCLIMB = .TRUE.
IMAGES = 5
ISTART = 0
NELM = 40
EDIFF = 1e-6
ISPIN = 1 ! polarization?
Ionic relaxation
NSW = 500 ! # of steps in optimization (default 0!)
ISIF = 2 ! 0: relax ions, 1,2:relax ions,calc stresses, 3:relax ion+cell
IBRION = 1 ! 1: quasi-NR, 2:CG algorithm for ions
NFREE = 40 ! number of DIIS vectors to save
POTIM = 0.5 ! reduce trial step in optimization
EDIFFG = -0.5
Dispersion
LVDW = .TRUE.
VDW_C6 = 42.440 1.750 0.700 0.140
VDW_R0 = 1.750 1.452 1.342 1.001
DOS
RWIGS = 1.300 0.770 0.730 0.320 ! Wigner-Seitz radii

```

### 1.3 Dimer Simulations

The following INCAR parameters are intended for dimer simulations in search for saddle points in VASP, for a system consists of Pt, C, O, and H atoms.

```

NWRITE = 1
LWAVE = .FALSE. ! write WAVECAR?
LCHARG = .FALSE. ! write CHGCAR?
LVTOT = .FALSE. ! write LOCPOT?
LSCAAWARE = .FALSE.
Electronic relaxation
IALGO = 48 ! 8: CG, 48: DIIS algorithm for electrons
ENCUT = 400
ALGO = Fast
ISMEAR = 0 ! 0: Gaussian, electron smearing
SIGMA = 0.100
PREC = normal
LREAL = Auto

```

```

ISTART = 0
NELM = 40
EDIFF = 1e-7
ISPIN = 1 ! polarization?
Ionic relaxation
NSW = 500 ! # of steps in optimization (default 0!)
ISIF = 2 ! 0: relax ions, 1,2:relax ions,calc stresses, 3:relax ion+cell
IBRION = 3 ! 1: quasi-NR, 2:CG algorithm for ions
NFREE = 4 ! number of DIIS vectors to save
EDIFFG = -0.03
Dimer setup
ICHAIN = 2
IOPT = 2
POTIM = 0.0 ! reduce trial step in optimization
DRotMax = 1 ! max rotation step each dimer iteration
Dispersion
LVDW = .TRUE.
VDW_C6 = 42.440 1.750 0.700 0.140
VDW_R0 = 1.750 1.452 1.342 1.001
DOS
RWIGS = 1.300 0.770 0.730 0.320 ! Wigner-Seitz radii

```

## 1.4 Vibrational Mode Simulations

The following INCAR parameters are intended for vibrational mode simulations in calculating vibrational frequencies in VASP, for a system that is previously converged from dimer calculations.

```

NWRITE = 1
LWAVE = .FALSE. ! write WAVECAR?
LCHARG = .FALSE. ! write CHGCAR?
LVTOT = .FALSE. ! write LOCPOT?
Electronic relaxation
IALGO = 48 ! 8: CG, 48: DIIS algorithm for electrons
ENCUT = 400
ALGO = Fast
ISMEAR = 0 ! 0: Gaussian, electron smearing
SIGMA = 0.100
PREC = normal
LREAL = Auto
ISTART = 0
NELM = 40
EDIFF = 1e-6
ISPIN = 1 polarization?
Ionic relaxation
NSW = 1 ! # of steps in optimization (default 0!)
ISIF = 2 ! 0: relax ions, 1,2:relax ions,calc stresses, 3:relax ion+cell

```

IBRION = 5 ! 1: quasi-NR, 2:CG algorithm for ions

NFREE = 2 ! number of DIIS vectors to save

POTIM = 0.015 ! reduce trial step in optimization

EDIFFG = -0.03

Dispersion

LVDW = .TRUE.

VDW\_C6 = 42.440 1.750 0.700 0.140

VDW\_R0 = 1.750 1.452 1.342 1.001

DOS

RWIGS = 1.300 0.770 0.730 0.320 ! Wigner-Seitz radii

## 1.5 Influence of Dipole Correction on Energy Calculations

The effect of dipole correction on energy calculations were investigated within two non-water mediated aqueous phase reactions,  $\text{CHOH-COH-COH}^* + * \rightarrow \text{COH-COH-COH}^* + \text{H}^*$  and  $\text{COH-COH-CO}^* + * \rightarrow \text{CO-COH-CO}^* + \text{H}^*$ . Each adsorbate has 10 snapshots of different water configurations from MD. (See Main text Section 2.5). Table 1 lists the reaction energies,  $E_{\text{rxn}}^{\text{aq}}$ , and the activation energies,  $E_{\text{act}}^{\text{aq}}$  from single point calculations on those system snapshots. To compare the energies calculated without dipole correction, the dipole correction were applied in the z-direction to the cells with an artificially added vacuum gap to facilitate electronic structure convergence. We find that dipole corrections have up to a 0.1 eV influence on the calculated energetics.

Table 1: Reaction energies,  $E_{\text{rxn}}^{\text{aq}}$  and the activation energies under different settings. Letters in parenthesis: a, without dipole correction; b, with dipole correction and added vacuum gap

| Type | Reaction  | $E_{\text{rxn}}^{\text{aq}}(\text{a})$ | $E_{\text{act}}^{\text{aq}}(\text{a})$ | $E_{\text{rxn}}^{\text{aq}}(\text{b})$ | $E_{\text{act}}^{\text{aq}}(\text{b})$ |
|------|---|--|--|--|--|
| CH   | $\text{CHOH-COH-COH}^* + * \rightarrow \text{COH-COH-COH}^* + \text{H}^*$ | -0.35                                  | 0.45                                   | -0.34                                  | 0.55                                   |
| OH   | $\text{COH-COH-CO}^* + * \rightarrow \text{CO-COH-CO}^* + \text{H}^*$     | 0.26                                   | 0.66                                   | 0.37                                   | 0.74                                   |

## 1.6 Influence of the D2 Dispersion Method on Reactions Energies

We selected 7 reactions in the methanol dehydrogenation network in the vacuum phase, and calculated the reaction energies with and without D2 dispersion correction<sup>1</sup> are listed in Table 2. The results indicate that this dispersion method has limited influence on the reaction energies.

Table 2: Reaction energies of methanol dehydrogenation in the vacuum phase, with and without D2 dispersion correction. Energy in eV unit.

| Reaction   | $\Delta E_{\text{rxn}} \text{ w D2}$ | $\Delta E_{\text{rxn}} \text{ w/o D2}$ |
|--|--------------------------------------|--|
| $\text{CH}_3\text{OH}^* + * \rightarrow \text{CH}_3\text{O}^* + \text{H}^*$  | -0.85                                | -0.80                                  |
| $\text{CH}_3\text{OH}^* + * \rightarrow \text{CH}_2\text{OH}^* + \text{H}^*$ | -1.97                                | -1.89                                  |
| $\text{CH}_2\text{OH}^* + * \rightarrow \text{CHOH}^* + \text{H}^*$          | 0.19                                 | 0.16                                   |
| $\text{CHOH}^* + * \rightarrow \text{COH}^* + \text{H}^*$                    | -1.09                                | -1.06                                  |
| $\text{CHOH}^* + * \rightarrow \text{CHO}^* + \text{H}^*$                    | -0.11                                | -0.05                                  |
| $\text{CHO}^* + * \rightarrow \text{CO}^* + \text{H}^*$                      | -0.85                                | -0.84                                  |
| $\text{COH}^* + * \rightarrow \text{CO}^* + \text{H}^*$                      | 0.14                                 | 0.17                                   |

## 2 Determination of the Size of Simulation Supercell

The volume of surface species was estimated by summing the total van der Waals volumes of each atom in the surface species using the van der Waals radii reported in<sup>2</sup>. We use the NPT ensemble to determine the size of our simulation supercell, with our desired pressure at 50 bar and temperature at 500K. We use a gradual temperature heating routine to equilibrate the system with liquid water, inspired by the work of Christopher O'Brien.<sup>3</sup> In our study a fixed amount of water, N=2880, are slowly heated to the target 500K temperature as the pressure is maintained around 50 bar. As reported in<sup>3</sup>, the key step is to slowly increase the temperature in NPT runs. We equilibrated the water structure starting at 100K and going to 500 K at intervals of 100 K. At temperature point along the way, we used a 0.5 fs timestep and ran the system for 60 ps to ensure water equilibration. We find that this 2880 water system has an average volume of 100389.58 Å<sup>3</sup> when equilibrated at 500K and 50 bar. For our DFT calculations, we ultimately use a system comprising 36 water molecules. Scaling down, this system should have a volume of 1254.87 Å<sup>3</sup> to give the same bulk density.

Next we evaluate the water bulk density for our aqueous catalytic system, to make sure it stays in the liquid phase. Here we consider that the supercell consists of two regions: a water-inaccessible region and water-accessible region. The water-inaccessible region includes the region enclosed by the van der Waals volumes of the surface adsorbate and the metal surface (using van der Waals radii reported in Ref.<sup>2</sup>). The water accessible region is where water can move freely without entering the volume occupied by the surface species and the Pt surface. We use this water-accessible region to determine the water density. In our supercells, the water-accessible volume is 1251.93 Å<sup>3</sup>, which corresponds to a bulk water density of 859 kg/m<sup>3</sup>, which is close to both the density of saturated liquid water as calculated with the TIP4P/2005 force field at 500 K of 0.850 g/cm<sup>3</sup><sup>4</sup>, and the experimental densities of saturated water at 500K of 0.844 g/cm<sup>3</sup><sup>5</sup>, and 837 kg/m<sup>3</sup><sup>6</sup>.

### 3 Pairwise Lennard Jones Parameters

Table 3: Lennard Jones potential coefficients. Atom identification is in bold in the second column for clarity.

| Atom | Specification                  | Force Field             | M(g/mol) | $\sigma_i$ (Å) | $\epsilon_i$ (Kcal/mol) |
|------|--------------------------------|-------------------------|----------|----------------|-------------------------|
| Pt   | Pt metal atoms                 | INTERFACE <sup>7</sup>  | 195.084  | 2.896          | 6.38                    |
| C    | Alcohol R <b>CH</b> 2OH        | OPLS-AA <sup>8</sup>    | 12.011   | 3.5            | 0.066                   |
| C    | Alcohol R2 <b>CHOH</b>         | OPLS-AA                 | 12.011   | 3.5            | 0.066                   |
| C    | Alcohol R3 <b>COH</b>          | OPLS-AA                 | 12.011   | 3.5            | 0.066                   |
| O    | Alcohol - <b>OH</b>            | OPLS-AA                 | 15.999   | 3.12           | 0.17                    |
| H    | Alcohol - <b>OH</b>            | OPLS-AA                 | 1.008    | 0              | 0                       |
| C    | Diol & Triol - <b>CH</b> 2OH   | OPLS-AA                 | 12.011   | 3.5            | 0.066                   |
| C    | Diol & Triol - <b>CH</b> ROH   | OPLS-AA                 | 12.011   | 3.5            | 0.066                   |
| C    | Diol & Triol - <b>CR</b> 2OH   | OPLS-AA                 | 12.011   | 3.5            | 0.066                   |
| O    | Diol - <b>OH</b>               | OPLS-AA                 | 15.999   | 3.07           | 0.17                    |
| O    | Triol - <b>OH</b>              | OPLS-AA                 | 15.999   | 3.07           | 0.17                    |
| H    | Diol - <b>OH</b>               | OPLS-AA                 | 1.008    | 0              | 0                       |
| H    | Triol - <b>OH</b>              | OPLS-AA                 | 1.008    | 0              | 0                       |
| H    | Diol & Triol H-COH             | OPLS-AA                 | 1.008    | 2.5            | 0.03                    |
| C    | Ethyl Ether -CH2OR             | OPLS-AA                 | 12.011   | 3.5            | 0.066                   |
| C    | Isopropyl Ether > <b>CH</b> OR | OPLS-AA                 | 12.011   | 3.5            | 0.066                   |
| C    | t-Butyl Ether COR              | OPLS-AA                 | 12.011   | 3.5            | 0.066                   |
| O    | Ether ROR                      | OPLS-AA                 | 15.999   | 3.07           | 0.17                    |
| H    | Alkyl Ether H-COR              | OPLS-AA                 | 1.008    | 2.5            | 0.03                    |
| C    | Ketone C=O                     | OPLS-AA                 | 12.011   | 3.5            | 0.066                   |
| O    | Ketone C=O                     | OPLS-AA                 | 15.999   | 3.07           | 0.17                    |
| O    | Water H-O-H                    | TIP4P/2005 <sup>9</sup> | 15.999   | 3.1589         | 0.1852                  |
| H    | Water H-O-H                    | TIP4P/2005              | 1.008    | 0              | 0                       |

Table 4: Pairwise Lennard Jones  $\epsilon$  coefficients with Lorentz-Berthelot mixing rules, in unit of Kcal/mol. Duplicates entries are marked with hyphens.

| Atom                  | Pt   | C       | O (Adsorbate) | Water O | Hydroxyl H (Adsorbate) | Alkyl H | Water H |
|-----------------------|------|---------|---------------|---------|------------------------|---------|---------|
| Pt                    | 6.38 | 0.64891 | 1.04144       | 1.087   | 0                      | 0.43749 | 0       |
| C                     | -    | 0.066   | 0.1059        | 0.1002  | 0                      | 0.0445  | 0       |
| O(Adsorbate)          | -    | -       | 0.17          | 0.1608  | 0                      | 0.0714  | 0       |
| Water O               | -    | -       | -             | 0.1852  | 0                      | 0.0675  | 0       |
| Hydroxyl H(Adsorbate) | -    | -       | -             | -       | 0                      | 0       | 0       |
| Alkyl H               | -    | -       | -             | -       | -                      | 0.03    | 0       |
| Water H               | -    | -       | -             | -       | -                      | -       | 0       |

Table 5: Pairwise Lennard Jones  $\sigma$  coefficients with Lorentz-Berthelot mixing rules, in unit of Å. Duplicates entries are marked with hyphens.

| Atom                            | Pt     | C      | Alcoholic O | Triol and Diol /Ether/ Carbonyl O | Water O | Hydroxyl H (Adsorbate) | Water H | Alkyl H |
|---------------------------------|--------|--------|-------------|-----------------------------------|---------|------------------------|---------|---------|
| Pt                              | 2.8960 | 3.1980 | 3.0080      | 2.9830                            | 3.0275  | 1.4480                 | 1.4480  | 2.6980  |
| Alcoholic/Triol/Diol C          | -      | 3.5000 | 3.3100      | 3.2850                            | 3.3295  | 1.7500                 | 1.7500  | 3.0000  |
| Alcoholic O                     | -      | -      | 3.1200      | 3.0950                            | 3.1395  | 1.5600                 | 1.5600  | 2.8100  |
| Triol and Diol/Ether/Carbonyl O | -      | -      | -           | 3.0700                            | 3.1145  | 1.5350                 | 1.5350  | 2.7850  |
| Water O                         | -      | -      | -           | -                                 | 3.1589  | 1.5795                 | 1.5795  | 2.8295  |
| Hydroxyl H                      | -      | -      | -           | -                                 | -       | 0.0000                 | 0.0000  | 1.2500  |
| Water H                         | -      | -      | -           | -                                 | -       | -                      | 0.0000  | 1.2500  |
| Alkyl H                         | -      | -      | -           | -                                 | -       | -                      | -       | 2.5000  |

## 4 Transition State Scaling

### 4.1 Building vacuum TSS with $E_{\text{bind}}$ from LSR

In this section, we derive linear equations that can be used to estimate the energies of catalytic species based on the TSS relationships that we derived in this work along with linear scaling relationships (LSRs) that we derived in our prior work<sup>10</sup>. We begin with the final state species. The binding energy of this species is calculated as

$$E_{\text{bind}}(\text{FS}) = E(\text{FS}^*) - E(*) - E_{\text{gas}}(\text{FS}) \quad (1)$$

where  $E_{\text{gas}}(\text{FS})$  is the electronic energy of the non-adsorbed final state molecule, which is commonly calculated by placing the species in an isolated supercell. Combining this equation with the definition of  $E(\text{FS})$ , i.e., the energy of  $\text{FS}^*$  relative to the energy of IS (g) plus the energy of the clean Pt(111) surface:

$$E(\text{FS}) = E_{\text{bind}}(\text{FS}) - E(*) - E_{\text{gas}}(\text{IS}) \quad (2)$$

and

$$E(\text{FS}) = E_{\text{bind}}(\text{FS}) + E_{\text{gas}}(\text{FS}) - E_{\text{gas}}(\text{IS}) \quad (3)$$

While,  $E(\text{IS})$  by definition is equal to  $E_{\text{bind}}(\text{IS})$ ,  $E(\text{TS})$  which is often hard to obtain, can be accessed through an existing TSS,

$$E(\text{TS}) = aE(\text{FS}) + b \quad (4)$$

where  $a$  and  $b$  are linear fitting parameters.

The reaction energy now can be expressed in terms of  $E(\text{FS})$  and  $E(\text{IS})$ , also in terms of  $E_{\text{bind}}(\text{FS})$  and  $E_{\text{bind}}(\text{IS})$

$$\Delta E_{\text{rxn}} = E(\text{FS}) - E(\text{IS}) = E_{\text{bind}}(\text{FS}) - E_{\text{bind}}(\text{IS}) + E_{\text{gas}}(\text{FS}) - E_{\text{gas}}(\text{IS}) \quad (5)$$

Then the activation energy can be calculated by,

$$E_{\text{act}} = E(\text{TS}) - E(\text{IS}) = aE(\text{FS}) + b - E_{\text{bind}}(\text{IS}) \quad (6)$$

$$= a(E_{\text{bind}}(\text{FS}) + E_{\text{gas}}(\text{FS}) - E_{\text{gas}}(\text{IS})) + b - E_{\text{bind}}(\text{IS}) \quad (7)$$

where the binding energy of vacuum FS (product) and IS (reactant) species can be discussed in our previous work<sup>10</sup>.

## 4.2 Comparison of TSS of Dehydrogenation Reactions with Literature Values

The TSS relationship that we established in this work for estimating the energies of transition states in the dehydrogenation pathway under vacuum is given in Figure 1, along with four other TSS relationships from the literature. The numbers after the authors' names indicate the year of publication. Murzin et al.<sup>11</sup> used 9 reactions pertaining to C-H dehydrogenation and 9 different reactions pertaining to O-H dehydrogenation. After combining those results, they developed a TSS relationship in the form  $E_{TS} = 0.83 E_{FS} + 0.74$ . Sautet et al.<sup>12</sup> studied 7 C-H type dehydrogenation reactions and 8 O-H type dehydrogenation reactions. Their TSS fit for the C-H type dehydrogenation was  $E_{TS} = 0.60 E_{FS} + 0.75$ . Vlachos et al.<sup>13</sup> studied 10 C-H type dehydrogenation reactions and 10 O-H type dehydrogenation reactions and arrived at the TSS fit of  $E_{TS} = 0.91 E_{FS} + 0.88$ . Greeley et al.<sup>14</sup> studied 10 C-H type dehydrogenation reactions and 8 O-H type dehydrogenation reactions and arrived at the TSS fit of  $E_{TS} = 1.05 E_{FS} + 1.04$ . Our TSS fit, determined from 5 C-H type and 2 O-H dehydrogenation reactions is  $E_{TS} = 1.10 E_{FS} + 1.18$ . The slope of this relationship is closest to Greeley's result. Our results also agree with Greeley's in that although C-H and O-H dehydrogenation reactions involve different bond types, they share a generic TSS relation.

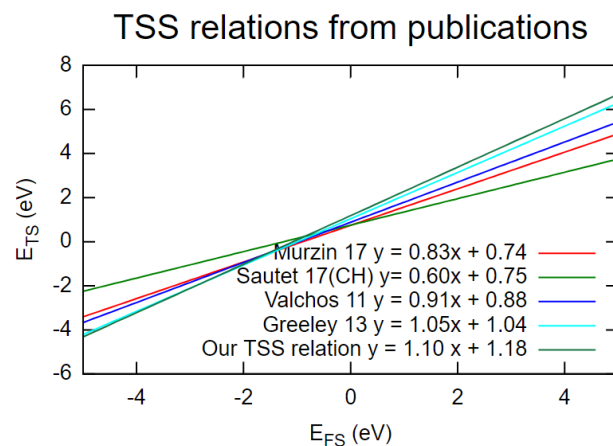


Figure 1: Comparison of TSS for vacuum dehydrogenation reactions in this work with literature.

## 4.3 Aqueous Phase TSS Relation

We define the aqueous final state energy  $E_{FS}^{aq}$  as,

$$E_{FS}^{aq} = E(FS^* + H_2O) - E(^* + H_2O) - E_{gas}(IS) \quad (8)$$

where the  $E(FS^* + H_2O)$  refers to the electronic energy of the product (commonly referred as final state species in TSS relations) under a specific  $H_2O$  configuration,  $E(^* + H_2O)$  refers to the electronic energy of the corresponding  $Pt + H_2O$  system with the catalytic species removed, and  $E_{gas}(IS)$  is the energy of the reactant species in gas phase.

Analogously, the transition state energy in the aqueous phase is written

$$E_{TS}^{aq} = E(TS^* + H_2O) - E(^* + H_2O) - E_{gas}(IS) \quad (9)$$

We have previously defined the interaction energy for a surface species under water,  $E_{int}$ <sup>10,15</sup>. For example,  $E_{int}$  for an arbitrary final state species  $FS^*$  in the vacuum phase is,

$$E_{int}(FS^*) = E(FS^* + H_2O) - E(^* + H_2O) + E(^*) - E(FS^*) \quad (10)$$

The electronic energy of the adsorbed final state species in the aqueous phase can then be written as the augmented vacuum electronic energy,

$$E_{FS}^{aq} = E_{FS}^{vac} + E_{int}(FS^*) \quad (11)$$

For the transition state and initial state species in the aqueous phase,

$$\begin{aligned} E_{\text{TS}}^{\text{aq}} &= E_{\text{TS}}^{\text{vac}} + E_{\text{int}}(\text{TS}^*) \\ E_{\text{IS}}^{\text{aq}} &= E_{\text{IS}}^{\text{vac}} + E_{\text{int}}(\text{IS}^*) \end{aligned} \quad (12)$$

We calculate electronic energies of species under liquid water by averaging over 10 frames that have been sampled from the MD trajectory<sup>10,15</sup>. Once several values for  $E_{\text{FS}}^{\text{aq}}$  and  $E_{\text{TS}}^{\text{aq}}$  are determined, an aqueous phase transition state scaling (TSS) relationship can be established through regression<sup>13,16–22</sup>.

## 5 MD/DFT Method: Full versus Simplified Methods

The following steps comprise a multiscale molecular dynamics/density functional theory (MD/DFT) method. It is based off prior work from our group<sup>10,15</sup>,

- (1) Structures of catalytic intermediates involved in the reactions listed in section 3.1 in the main text are generated and optimized under vacuum using DFT. Transition states for the reactions are found using a combination of the NEB<sup>23,24</sup> and dimer<sup>25</sup> methods, and their identities are confirmed through their vibrational frequencies.
- (2) 36 H<sub>2</sub>O molecules are added to the simulation cells. MD is run, allowing the H<sub>2</sub>O molecules to move. MD simulations are carried out for 5 ns, the first 2 ns are intended for system equilibration, and the final 3 ns are used for configurational sampling.
- (3) 10 different configurations of H<sub>2</sub>O molecules are extracted from the production run of the MD trajectory at constant time intervals of 300,000 fs.
- (4) The configurations are inspected for hydrogen bonding between the surface species and the H<sub>2</sub>O molecules. Hydrogen bonds are determined based on geometric criteria:<sup>26–29</sup> The distance between the donor and acceptor oxygen pair,  $d_{\text{O-D}}$ ,  $\leq 3.5$  Å; the angle between the donor, acceptor, and the participating proton,  $\angle \text{DAH}$ ,  $\leq 30^\circ$ ; and the angle between the acceptor, participating proton, and donor,  $\angle \text{AHD} \geq 120^\circ$ . The H<sub>2</sub>O molecules that hydrogen bond with the catalytic species are identified by a Python code available on GitHub<sup>30</sup>.
- (5) Partial relaxations are performed on the configurations using DFT. In these partial relaxations, the geometries of the adsorbates and the H<sub>2</sub>O molecules that are hydrogen bonded to them are relaxed, while the positions of all other atoms are held fixed. For transition states, we find that the quasi-Newton-Raphson optimizer is able to locate the transition state structures, avoiding the need to employ NEB or dimer in this step.
- (6) Interaction energies are calculated for the different species according to equation 10.
- (7) Reaction energies and activation energies are calculated based on equations 2 and 6 in the main text and are reported as averages.

This is the full method. In this full method, geometry optimizations in DFT are carried out twice: once for the surface species in vacuum and again after they are solvated in liquid water. The need to carry out a second round of DFT calculations can push the computational tractability of this approach, since there are multiple catalytic species in the APR reaction network. Further, it is observed that the geometries of the catalytic species and water molecules do not change dramatically during the second round of geometry optimizations. Based on this observation, in this paper, a simplified method was applied, where the second round of geometry optimization was omitted, meaning that steps 4 and 5 are eliminated, and instead DFT single point calculations were performed on the configurations that were sampled from the MD trajectories. Table 6 compares reaction and activation energies calculated by these two methods. With the exception of the activation energies of the third reaction, all differences are  $\leq 0.1$  eV.

Table 6: Activation energies of reactions by MD/DFT procedures with reoptimized and fixed adsorbates. Energies in eV.

| Number | Reaction   | $E_{rxn}^{aq}$ (MD/DFT) <sup>a</sup> | $E_{rxn}^{aq}$ (MD/DFT)(fixed) | $E_{act}^{aq}$ (MD/DFT) <sup>a</sup> | $E_{act}^{aq}$ (MD/DFT)(fixed) |
|--------|--|--------------------------------------|--------------------------------|--------------------------------------|--------------------------------|
| 1      | $\text{CH}_2\text{OH}-\text{CHOH}-\text{CH}_2\text{OH} \rightarrow \text{CH}_2\text{OH}-\text{COH}-\text{CH}_2\text{OH}$ | -0.52±0.12                           | -0.44±0.10                     | 0.32±0.14                            | 0.32±0.10                      |
| 2      | $\text{CH}_2\text{OH}-\text{COH}-\text{CH}_2\text{OH} \rightarrow \text{CHOH}-\text{COH}-\text{CH}_2\text{OH}$           | -0.42±0.15                           | -0.39±0.14                     | 0.44±0.14                            | 0.48±0.11                      |
| 3      | $\text{CHOH}-\text{COH}-\text{CH}_2\text{OH} \rightarrow \text{CHOH}-\text{COH}-\text{CHOH}$                             | -0.17±0.13                           | -0.10±0.10                     | 1.29±0.29                            | 1.11±0.10                      |
| 4      | $\text{CHOH}-\text{COH}-\text{CHOH} \rightarrow \text{COH}-\text{COH}-\text{CHOH}$                                       | -0.20±0.14                           | -0.11±0.11                     | 0.47±0.18                            | 0.48±0.14                      |
| 5      | $\text{COH}-\text{COH}-\text{CHOH} \rightarrow \text{COH}-\text{COH}-\text{COH}$   | -0.29±0.16                           | -0.38±0.12                     | 0.55±0.20                            | 0.45±0.14                      |
| 6      | $\text{COH}-\text{COH}-\text{COH} \rightarrow \text{CO-COH-COH}$   | 0.30±0.17                            | 0.24±0.10                      | 0.42±0.19                            | 0.38±0.12                      |
| 7      | $\text{CO-COH-COH} \rightarrow \text{CO-COH-CO}$   | 0.33±0.14                            | 0.26±0.09                      | 0.69±0.15                            | 0.66±0.08                      |

Note: superscript <sup>a</sup> denotes that the surface geometries have been optimized twice.

## 6 DFT Calculated Surface Geometries and Partial Charges

This section presents the cartesian coordinates and snapshots of the vacuum structures of all catalytic intermediates and transition states (dissociating atoms/groups are within parentheses) that were explicitly calculated with DFT for this work. In the coordinate lists, the coordinates of Pt atoms are omitted for simplicity. The partial charges on the atoms are included in the fourth columns of the coordinate lists. These were calculated using the DDEC packages<sup>31–36</sup>.

### 6.1 Pt Structure

The Cartesian coordinates for atoms of the Pt(111) surface are presented. For simplicity, Pt coordinates for all the surface species below are neglected. Note that the topmost layer (last 16 atoms) of the Pt(111) is allowed to optimize during non-single-point DFT simulations, the coordinates of them may vary among adsorbates, though the changes are often small.

Pt 1.42807 4.86095 0.00000

Pt 9.84241 4.86077 0.00000

Pt 8.44063 7.28856 0.00000

Pt 2.82987 7.28856 0.00000

Pt 0.02476 7.28856 0.00000

Pt 0.02530 2.43093 0.00000

Pt 4.23352 4.85904 0.00000

Pt 9.84351 0.00000 0.00000

Pt 5.63437 7.28633 0.00000

Pt 2.83226 2.43163 0.00000

Pt 1.42735 0.00000 0.00000

Pt 8.43883 2.42952 0.00000

Pt 7.03597 4.85904 0.00000

Pt 7.03790 0.00000 0.00000

Pt 4.23257 0.00000 0.00000

Pt 5.63500 2.43110 0.00000

Pt 9.84814 3.25324 2.25195

Pt 1.43175 3.25591 2.25158

Pt 8.44413 5.68280 2.25214

Pt 2.83510 5.68697 2.25077

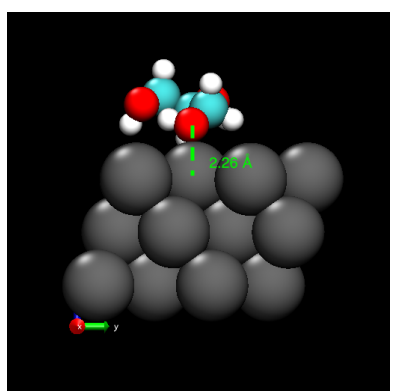
Pt 7.04141 8.11706 2.25171

Pt 8.44378 0.82528 2.25306

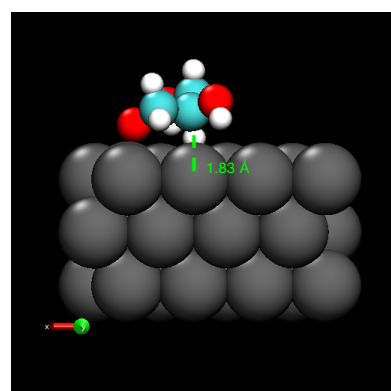
Pt 0.02786 0.82498 2.25321  
Pt 2.83263 0.83014 2.25307  
Pt 4.23522 8.12048 2.25248  
Pt 5.63801 0.83076 2.25249  
Pt 9.84674 8.11305 2.25253  
Pt 1.43075 8.11450 2.25283  
Pt 5.63916 5.68945 2.25153  
Pt 0.02965 5.68344 2.25239  
Pt 7.04332 3.25564 2.25239  
Pt 4.23688 3.26012 2.25258  
Pt 7.04456 6.51616 4.50228  
Pt 8.44804 4.08541 4.50644  
Pt 2.83553 4.08655 4.50482  
Pt 4.23731 6.51699 4.50357  
Pt 5.64279 4.08937 4.50316  
Pt 9.84710 1.65501 4.50634  
Pt 7.04193 1.65726 4.50665  
Pt 4.23794 1.65949 4.50572  
Pt 1.43193 1.65772 4.50661  
Pt 0.03002 4.08419 4.50663  
Pt 9.84987 6.51233 4.50392  
Pt 5.63949 8.94561 4.50501  
Pt 8.44582 8.94351 4.50557  
Pt 1.43387 6.51306 4.50507  
Pt 0.02952 8.94268 4.50638  
Pt 2.83329 8.94659 4.50583

## 6.2 CH<sub>2</sub>OH-CHOH-CH<sub>2</sub>OH

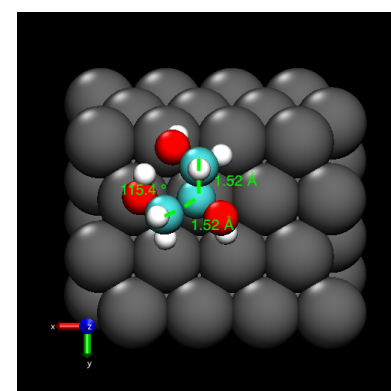
C 7.111599 4.716601 7.531633 -0.019722  
C 5.744697 4.043197 7.418093 0.177871  
C 5.634541 2.670712 8.073425 0.002560  
O 8.163540 3.973100 6.853611 -0.327407  
O 4.693530 4.857883 7.846094 -0.444273  
O 6.764658 1.846406 7.734654 -0.424801  
H 7.400246 4.805376 8.593669 0.113339  
H 7.968744 3.015481 7.080143 0.335645  
H 4.483396 5.496331 7.125705 0.320758  
H 4.688245 2.200076 7.757481 0.085433  
H 7.072976 5.719312 7.076902 0.087648  
H 5.631298 2.783530 9.170135 0.107440  
H 6.562468 1.378402 6.881984 0.287667  
H 5.603448 3.791440 6.293991 0.004322



(a) Front view of  $\text{CH}_2\text{OH}-\text{CHOH}-\text{CH}_2\text{OH}$



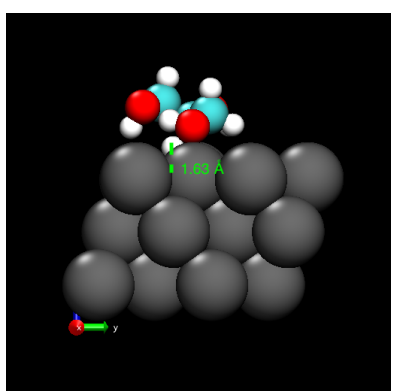
(b) Side view of  $\text{CH}_2\text{OH}-\text{CHOH}-\text{CH}_2\text{OH}$



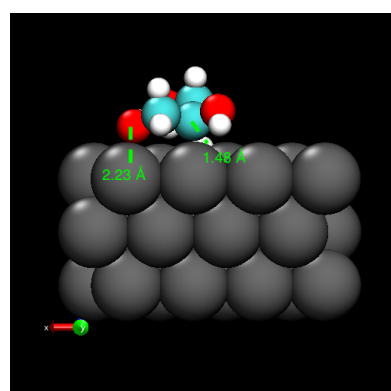
(c) Top view of  $\text{CH}_2\text{OH}-\text{CHOH}-\text{CH}_2\text{OH}$

### 6.3 $\text{CH}_2\text{OH}-\text{C}(\text{H})\text{OH}-\text{CH}_2\text{OH}$

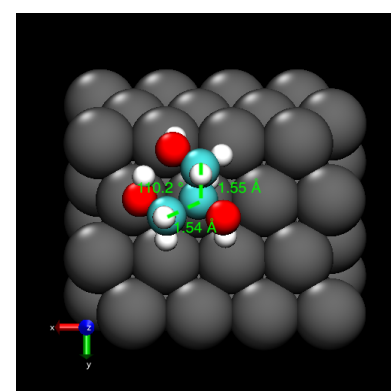
```
C 7.001072 4.722510 7.275243 -0.023787
C 5.652337 4.035772 7.013421 0.205186
C 5.576832 2.691908 7.787041 -0.004183
O 8.154529 4.014295 6.772142 -0.315330
O 4.582555 4.798933 7.427566 -0.412126
O 6.740084 1.891721 7.601665 -0.406717
H 7.109467 4.790536 8.374875 0.114408
H 7.985677 3.059338 7.026363 0.340132
H 4.498600 5.595281 6.840645 0.320967
H 4.655491 2.147870 7.521977 0.094433
H 7.021595 5.738272 6.843978 0.089994
H 5.540375 2.964403 8.855515 0.118622
H 6.645772 1.395740 6.735870 0.276290
H 5.250167 3.186810 5.875577 0.034036
```



(a) Front view of  $\text{CH}_2\text{OH}-\text{C}(\text{H})\text{OH}-\text{CH}_2\text{OH}$



(b) Side view of  $\text{CH}_2\text{OH}-\text{C}(\text{H})\text{OH}-\text{CH}_2\text{OH}$



(c) Top view of  $\text{CH}_2\text{OH}-\text{C}(\text{H})\text{OH}-\text{CH}_2\text{OH}$

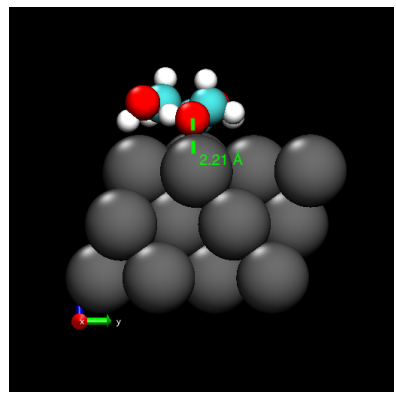
### 6.4 $\text{CH}_2\text{OH}-\text{COH}-\text{CH}_2\text{OH}$

```
C 7.092927 4.834170 7.278256 -0.029001
C 5.739805 4.205683 6.895794 0.163312
C 5.579154 2.842023 7.607463 -0.000543
O 8.229407 4.086063 6.769312 -0.303673
O 4.682623 4.979135 7.383282 -0.417342
O 6.770830 2.041739 7.599725 -0.413173
H 7.175379 4.836250 8.381381 0.115086
H 8.008736 3.140815 7.041885 0.332940
H 4.616588 5.806843 6.844594 0.317807
H 4.719350 2.290114 7.192816 0.084260
```

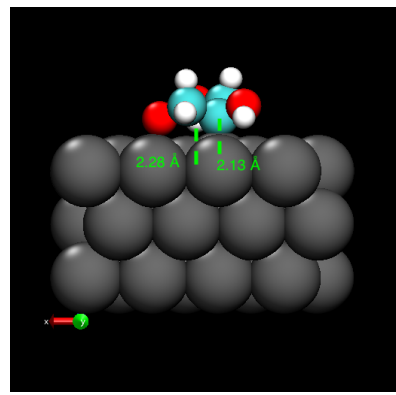
H 7.178139 5.867465 6.901547 0.093469

H 5.371376 3.068843 8.666601 0.112386

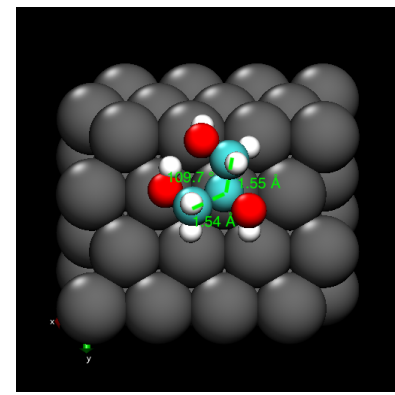
H 6.754369 1.459597 6.790244 0.287005



(a) Front view of  $\text{CH}_2\text{OH}-\text{COH}-\text{CH}_2\text{OH}$



(b) Side view of  $\text{CH}_2\text{OH}-\text{COH}-\text{CH}_2\text{OH}$



(c) Top view of  $\text{CH}_2\text{OH}-\text{COH}-\text{CH}_2\text{OH}$

## 6.5 HC(H)OH-COH-CH<sub>2</sub>OH

C 6.943767 4.404855 7.343054 -0.004274

C 5.586717 3.895336 6.759493 0.107085

C 5.282899 2.524329 7.269537 0.209771

O 8.161699 3.858184 6.796897 -0.321874

O 4.576047 4.716893 7.307082 -0.438141

O 6.160725 1.563804 7.349591 -0.281713

H 6.953451 4.227928 8.432767 0.108542

H 8.181718 2.882683 6.914194 0.343543

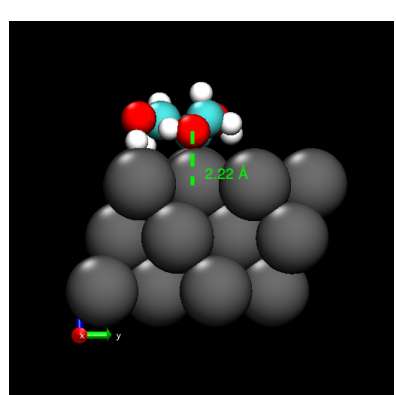
H 4.472668 5.509927 6.721664 0.310291

H 3.983042 1.822499 6.186744 -0.019307

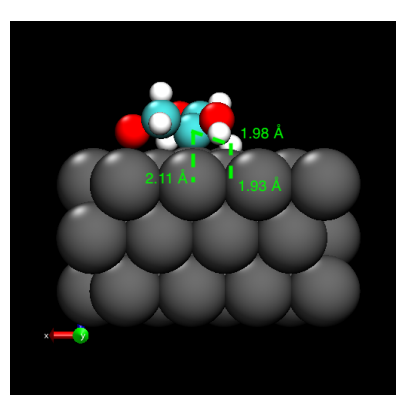
H 6.989470 5.483503 7.138702 0.104420

H 4.449699 2.454544 7.985225 0.127137

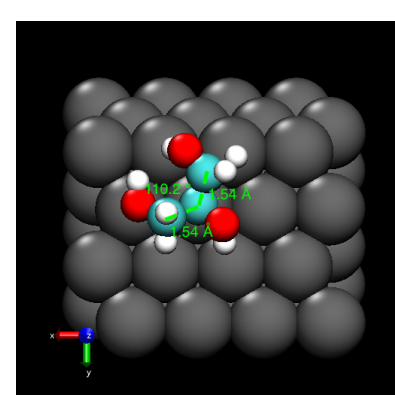
H 6.688322 1.482503 6.393800 0.205963



(a) Front view of  $\text{HC}(\text{H})\text{OH}-\text{COH}-\text{CH}_2\text{OH}$



(b) Side view of  $\text{HC}(\text{H})\text{OH}-\text{COH}-\text{CH}_2\text{OH}$



(c) Top view of  $\text{HC}(\text{H})\text{OH}-\text{COH}-\text{CH}_2\text{OH}$

## 6.6 CHOH-COH-CH<sub>2</sub>OH

C 6.851239 4.180892 7.345939 -0.015926

C 5.532823 3.753306 6.663480 0.146104

C 5.089282 2.292359 6.810374 0.075184

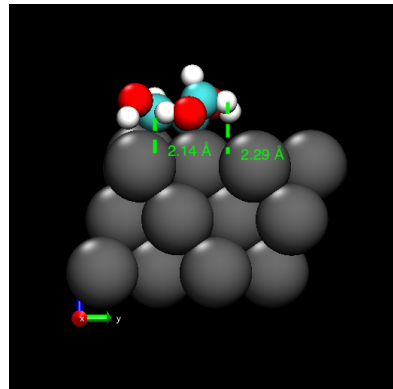
O 8.101982 3.711178 6.788080 -0.316188

O 4.508037 4.533610 7.236894 -0.424563

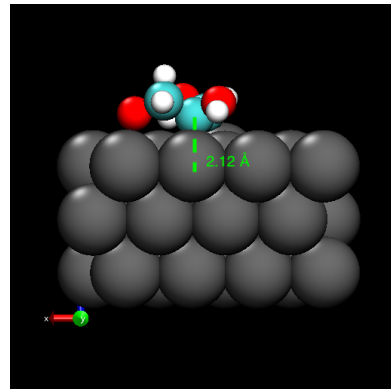
O 6.035319 1.417916 7.353243 -0.388873

H 6.818059 3.856376 8.399639 0.117490

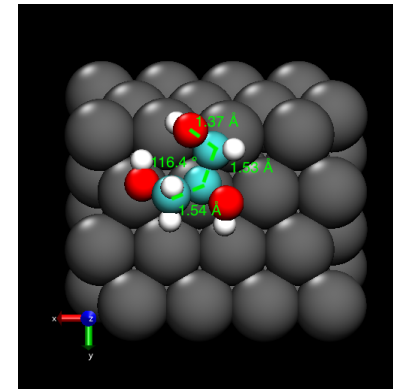
H 8.122875 2.729468 6.841141 0.334243  
 H 4.573522 5.450695 6.881269 0.330107  
 H 6.912068 5.276800 7.287775 0.099805  
 H 4.182338 2.244128 7.433116 0.122050  
 H 6.639578 1.104022 6.621879 0.273867



(a) Front view of  $\text{CHOH-COH-CH}_2\text{OH}$



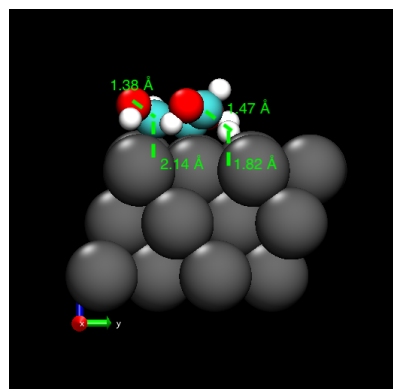
(b) Side view of  $\text{CHOH-COH-CH}_2\text{OH}$



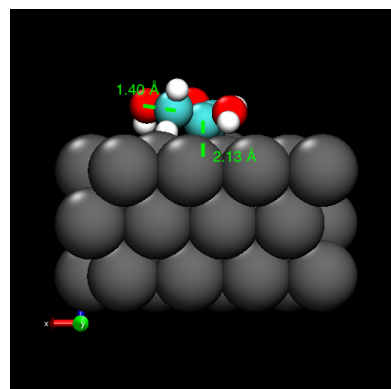
(c) Top view of  $\text{CHOH-COH-CH}_2\text{OH}$

## 6.7 $\text{CHOH-COH-C(H)}_2\text{OH}$

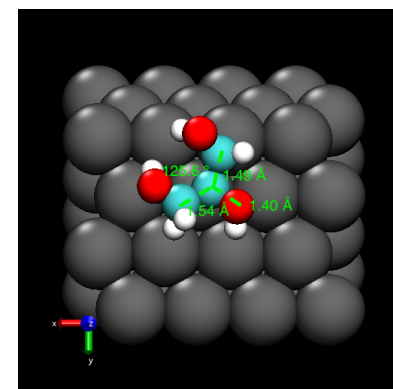
C 7.625911 4.470948 7.131846 0.120214  
 C 6.362185 3.869360 6.606785 0.158814  
 C 5.963090 2.385778 6.716331 0.076082  
 O 8.750620 3.746008 7.295627 -0.314800  
 O 5.242178 4.619139 6.991256 -0.387455  
 O 6.826878 1.501861 7.326147 -0.359239  
 H 7.474147 5.166266 7.969655 0.134643  
 H 8.864389 3.105130 6.531708 0.275176  
 H 5.299270 5.531122 6.590875 0.309724  
 H 7.926060 5.550675 6.176958 -0.014591  
 H 4.989516 2.335108 7.227147 0.119863  
 H 7.611043 1.353427 6.732561 0.295470



(a) Front view of  $\text{CHOH-COH-C(H)}_2\text{OH}$



(b) Side view of  $\text{CHOH-COH-C(H)}_2\text{OH}$

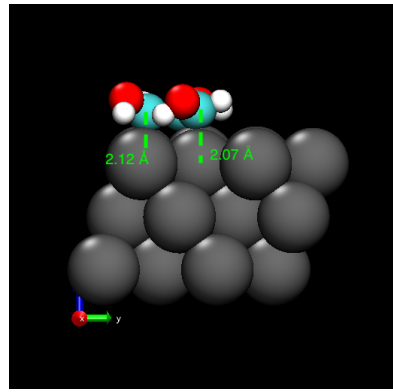


(c) Top view of  $\text{CHOH-COH-C(H)}_2\text{OH}$

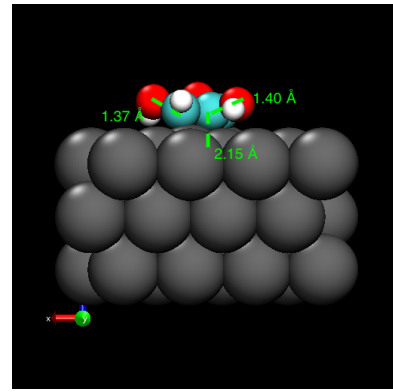
## 6.8 $\text{CHOH-COH-CHOH}$

C 3.892355 2.041146 6.564017 0.058872  
 C 3.694978 3.563094 6.540917 0.145964  
 C 4.967355 4.282018 6.291715 0.137513  
 O 4.942310 1.569411 7.351084 -0.372029  
 O 2.898875 3.985831 7.588201 -0.386583  
 O 5.433910 5.047162 7.258461 -0.277673

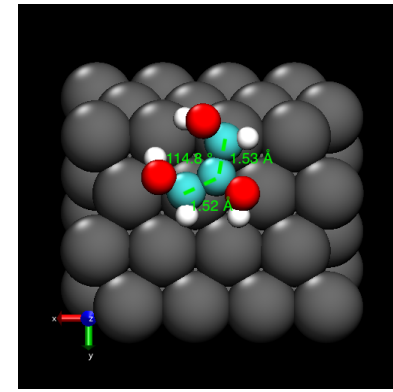
H 5.795640 1.837436 6.939211 0.323672  
 H 2.759511 4.952585 7.505322 0.369682  
 H 6.191807 5.576272 6.891719 0.353642  
 H 2.966717 1.573357 6.929648 0.110797  
 H 4.048292 6.922129 6.065634 -0.021995



(a) Front view of CHOH-COH-CHOH



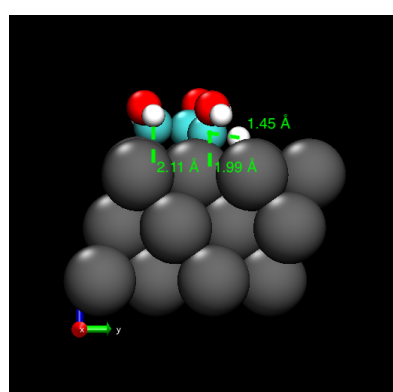
(b) Side view of CHOH-COH-CHOH



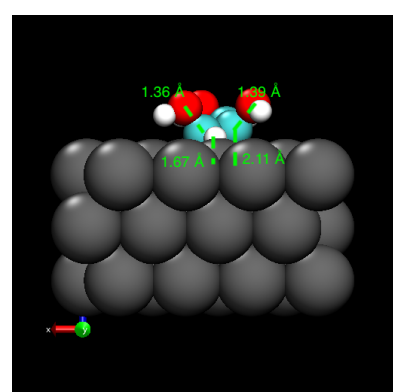
(c) Top view of CHOH-COH-CHOH

## 6.9 C(H)OH-COH-CHOH

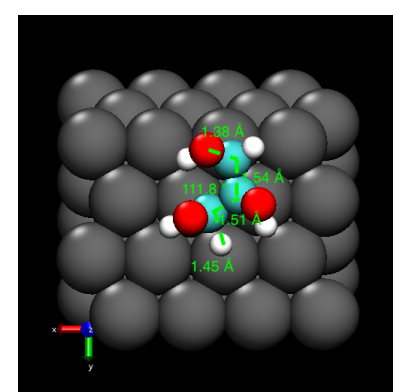
C 3.903935 2.285673 6.592792 0.072569  
 C 3.626856 3.797378 6.456973 0.141838  
 C 4.902430 4.586933 6.256737 0.105812  
 O 4.970283 1.888660 7.380657 -0.356704  
 O 2.764369 4.232437 7.455757 -0.389469  
 O 5.671166 4.792820 7.355274 -0.317313  
 H 5.798591 2.287830 7.032800 0.330664  
 H 2.459092 5.136325 7.222422 0.355818  
 H 6.528536 5.172068 7.046611 0.356288  
 H 2.997417 1.798223 6.979842 0.112163  
 H 4.369144 5.926065 6.079419 0.026887



(a) Front view of C(H)OH-COH-CHOH



(b) Side view of C(H)OH-COH-CHOH



(c) Top view of C(H)OH-COH-CHOH

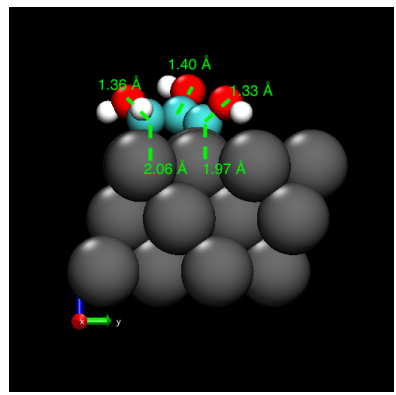
## 6.10 COH-COH-CHOH

C 5.318817 1.967221 6.563483 0.019602  
 C 4.953463 3.425700 6.680538 0.207687  
 C 5.996147 4.383815 6.313371 0.137750  
 O 4.341787 1.218151 7.240364 -0.428927  
 O 4.100122 3.750546 7.683705 -0.368580  
 O 6.207942 5.352202 7.201148 -0.284047  
 H 4.266943 0.329997 6.817134 0.336890

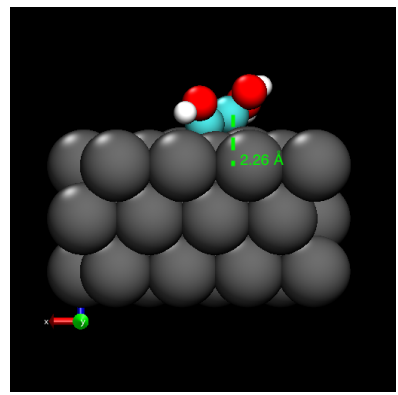
H 3.614827 2.917863 7.900695 0.385041

H 6.819517 6.018425 6.796042 0.340528

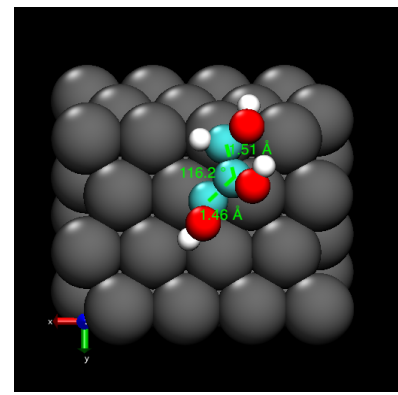
H 6.336187 1.771353 6.950213 0.101682



(a) Front view of COH-COH-CHOH



(b) Side view of COH-COH-CHOH



(c) Top view of COH-COH-CHOH

## 6.11 COH-COH-C(H)OH

C 6.074222 1.814200 6.531571 0.051655

C 6.167278 3.068289 7.208064 0.203834

C 6.716520 4.200678 6.533146 0.115833

O 5.681669 0.807145 7.373581 -0.384324

O 5.861496 3.166743 8.513570 -0.346417

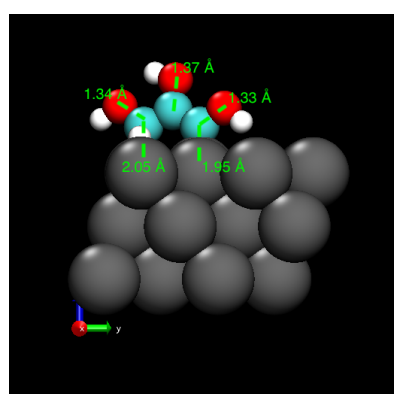
O 6.991535 5.242330 7.306630 -0.277655

H 5.486615 0.006531 6.827086 0.340820

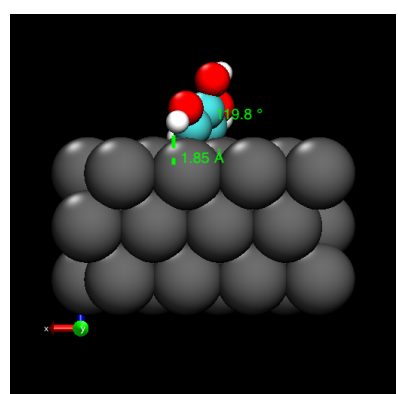
H 5.492888 2.300065 8.798699 0.383445

H 7.339294 5.976375 6.725530 0.319232

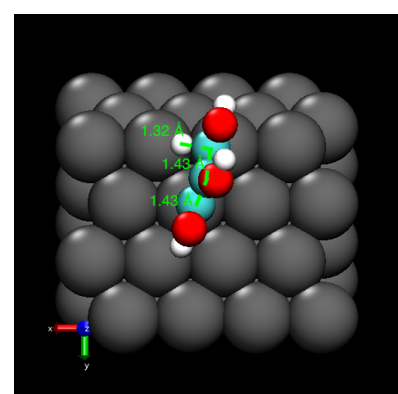
H 7.305138 1.647758 6.071909 0.043778



(a) Front view of COH-COH-C(H)OH



(b) Side view of COH-COH-C(H)OH



(c) Top view of COH-COH-C(H)OH

## 6.12 COH-COH-COH

C 4.419481 1.793481 6.603704 0.126861

C 5.105440 2.841352 7.268349 0.131145

C 5.703729 3.896114 6.548531 0.088890

O 3.895755 0.869962 7.402160 -0.283837

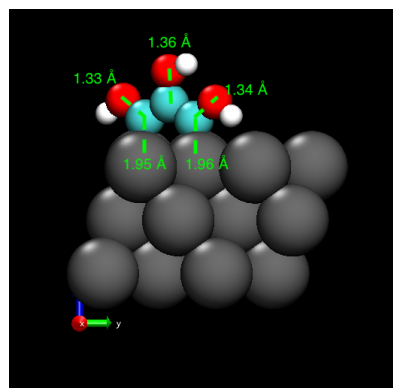
O 5.178870 2.799633 8.630260 -0.372184

O 6.337241 4.788962 7.322905 -0.338254

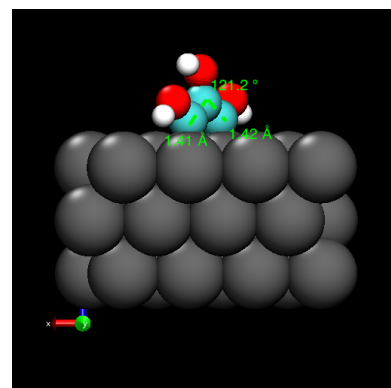
H 6.753808 5.480704 6.733884 0.330714

H 3.462637 0.175567 6.839778 0.328793

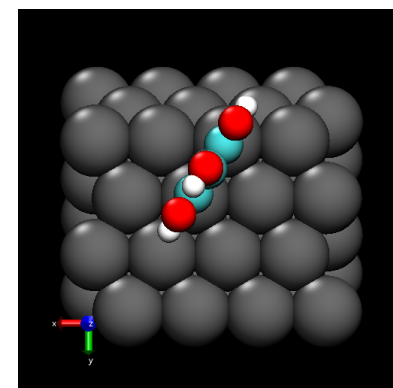
H 5.712796 3.565135 8.928035 0.375779



(a) Front view of COH-COH-COH



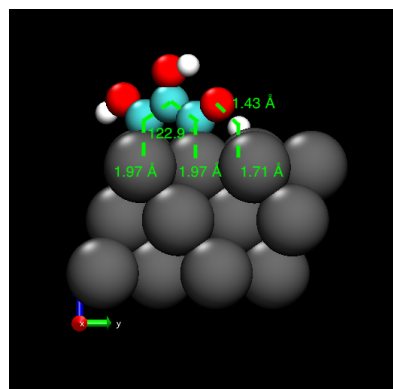
(b) Side view of COH-COH-COH



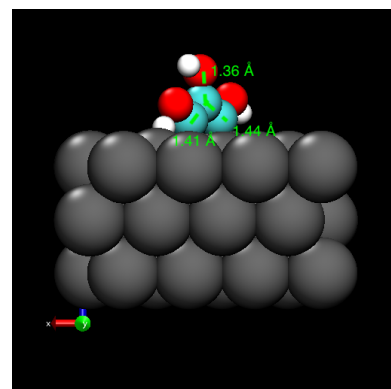
(c) Top view of COH-COH-COH

### 6.13 COH-COH-CO(H)

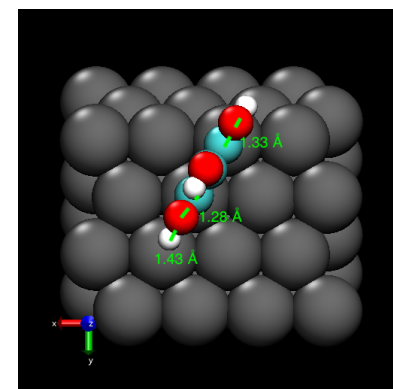
```
C 4.419582 1.802004 6.594733 0.109468
C 5.090886 2.860001 7.244244 0.134306
C 5.671245 3.968921 6.534813 0.115798
O 3.893522 0.879710 7.401429 -0.292566
O 5.173528 2.841663 8.599148 -0.353323
O 6.225425 4.905190 7.201490 -0.266279
H 6.723219 5.822450 6.221972 0.126382
H 3.460461 0.180727 6.846922 0.330396
H 5.664220 3.649197 8.868549 0.371644
```



(a) Front view of COH-COH-CO(H)



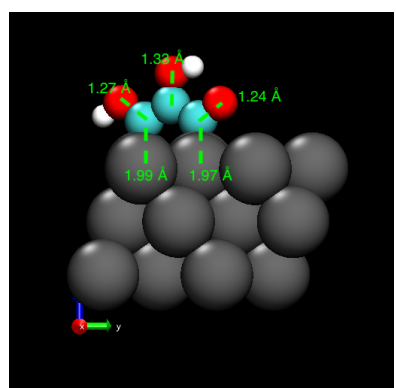
(b) Side view of COH-COH-CO(H)



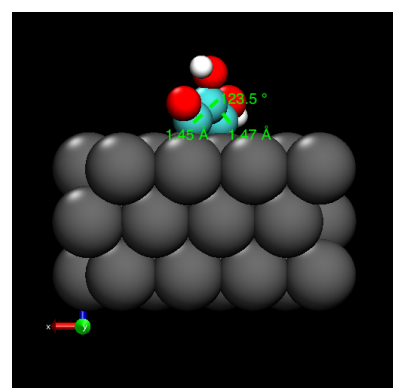
(c) Top view of COH-COH-CO(H)

### 6.14 COH-COH-CO

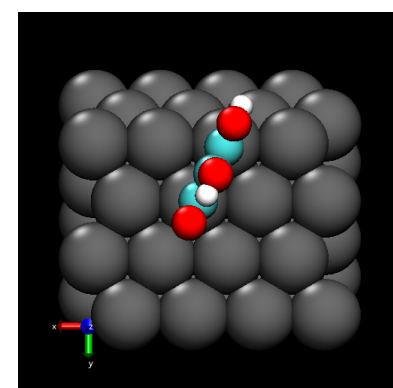
```
C 4.324193 1.757203 6.573869 0.093589
C 4.784970 2.900458 7.254083 0.151680
C 5.421938 4.056491 6.617582 0.150256
O 3.897606 0.761402 7.352603 -0.287444
O 4.680806 2.943936 8.598874 -0.335491
O 5.805088 4.993333 7.321011 -0.312701
H 5.060881 3.812266 8.874552 0.371878
H 3.577517 0.020321 6.773078 0.322835
```



(a) Front view of COH-COH-CO



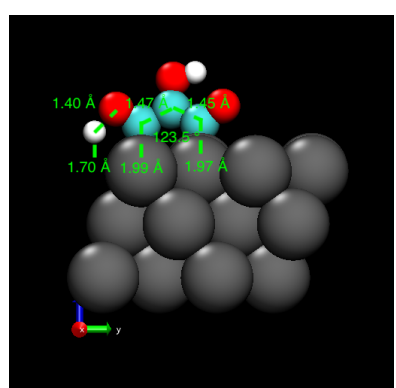
(b) Side view of COH-COH-CO



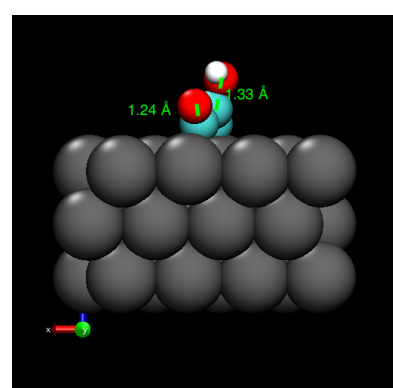
(c) Top view of COH-COH-CO

## 6.15 CO(H)-COH-CO

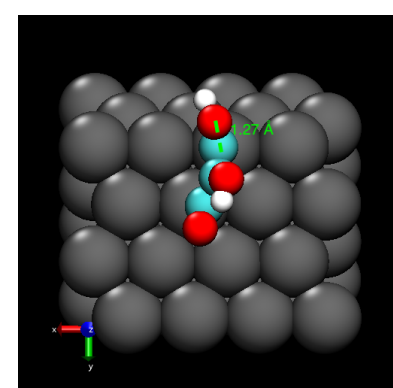
C 4.569438 1.623434 6.532507 0.138574  
 C 4.567654 2.916211 7.178024 0.188342  
 C 5.161724 4.124226 6.579416 0.128725  
 O 4.737853 0.552133 7.184712 -0.202464  
 O 4.234010 2.986093 8.467871 -0.313290  
 O 5.351661 5.098862 7.314414 -0.314333  
 H 4.421680 3.919505 8.747179 0.381312  
 H 5.142705 9.346517 6.206724 0.127683



(a) Front view of CO(H)-COH-CO



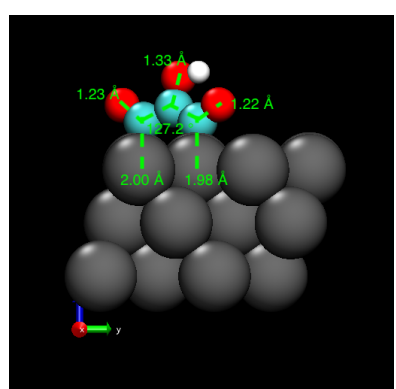
(b) Side view of CO(H)-COH-CO



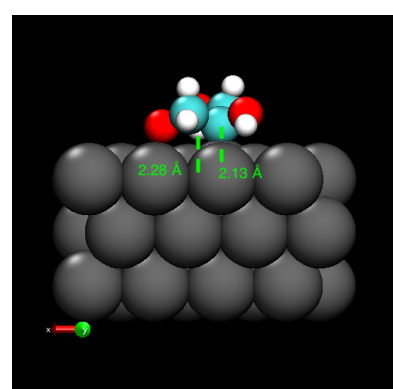
(c) Top view of CO(H)-COH-CO

## 6.16 CO-COH-CO

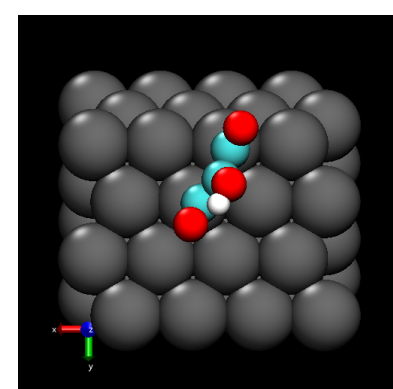
C 3.718329 2.112399 6.502695 0.202635  
 C 3.584654 3.655679 6.552389 0.118599  
 C 5.006639 4.232981 6.526960 0.236091  
 O 3.460057 1.377431 7.422864 -0.228963  
 O 2.840447 4.176684 7.579774 -0.366780  
 O 5.585494 4.719653 7.463267 -0.215230  
 H 1.942188 3.788758 7.543046 0.373869



(a) Front view of CO-COH-CO



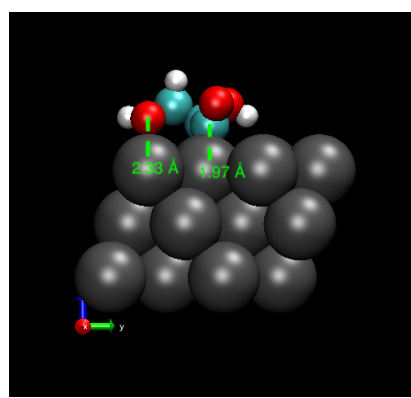
(b) Side view of CO-COH-CO



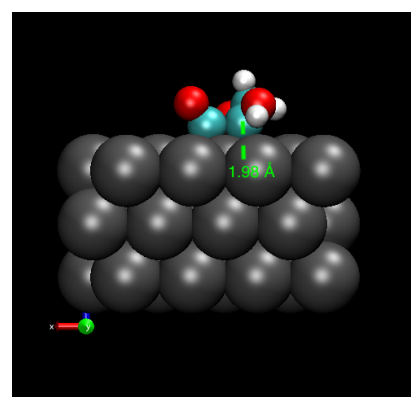
(c) Top view of CO-COH-CO

## 6.17 CO-CHOH-CH<sub>2</sub>OH

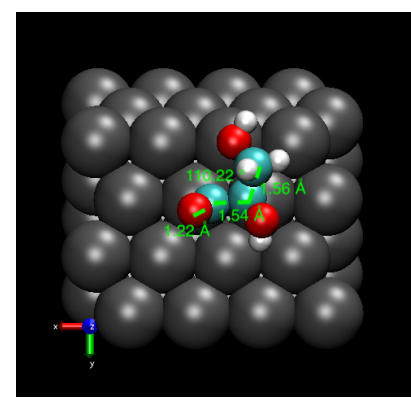
C 5.585629 3.824365 6.682182 0.194695  
C 4.218705 3.835667 7.435678 0.108582  
C 3.719406 2.392795 7.656009 0.015093  
O 6.570188 3.566107 7.353626 -0.296409  
O 3.154151 4.552103 6.800932 -0.348277  
O 4.332272 1.382980 6.826574 -0.349046  
H 3.454704 5.478858 6.584333 0.313758  
H 2.652328 2.360084 7.389457 0.117733  
H 3.857334 2.098609 8.706602 0.103419  
H 5.294872 1.316595 7.011398 0.357563  
H 4.421153 4.314671 8.408234 0.097600



(a) Front view of CO-CHOH-CH<sub>2</sub>OH



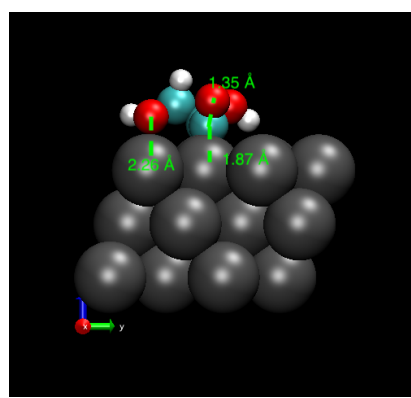
(b) Side view of CO-CHOH-CH<sub>2</sub>OH



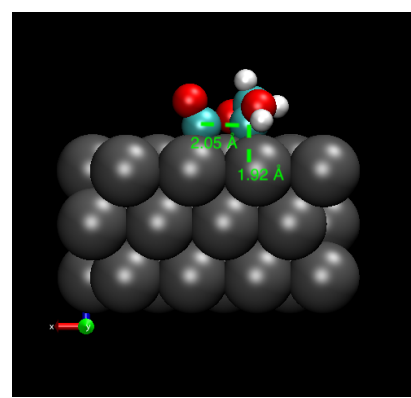
(c) Top view of CO-CHOH-CH<sub>2</sub>OH

## 6.18 (CO)-CHOH-CH<sub>2</sub>OH

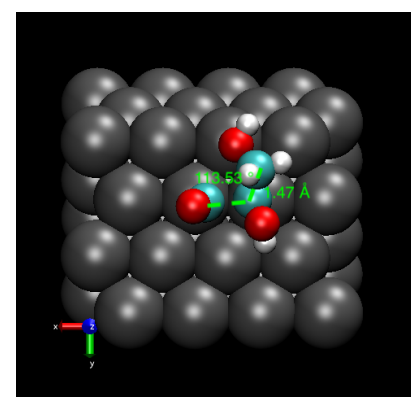
C 5.561852 3.807135 6.681133 0.196403  
C 4.190630 3.827825 7.427910 0.107073  
C 3.686069 2.385837 7.645276 0.017692  
O 6.534539 3.520860 7.359194 -0.299814  
O 3.130857 4.547924 6.787697 -0.343050  
O 4.311356 1.374991 6.826655 -0.344468  
H 3.431881 5.476788 6.579431 0.312909  
H 2.622290 2.352154 7.364359 0.116811  
H 3.810072 2.093993 8.698350 0.102399  
H 5.271656 1.314671 7.022393 0.353924  
H 4.388276 4.307305 8.400527 0.096841



(a) Front view of (CO)-CHOH-CH<sub>2</sub>OH



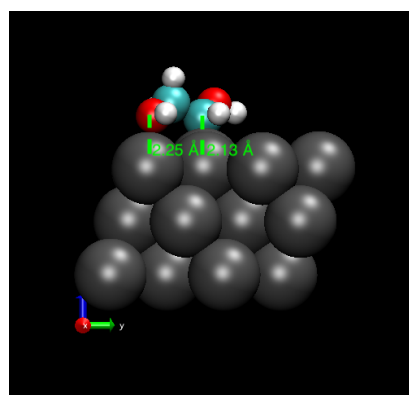
(b) Side view of (CO)-CHOH-CH<sub>2</sub>OH



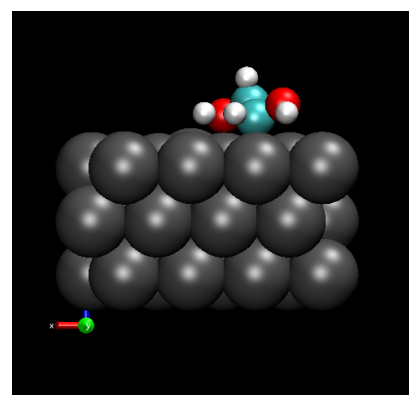
(c) Top view of (CO)-CHOH-CH<sub>2</sub>OH

## 6.19 CHOH-CH<sub>2</sub>OH

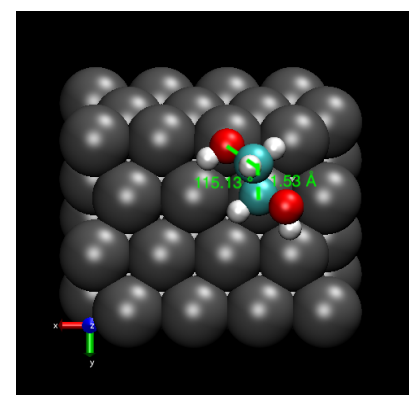
C 2.884770 4.025267 6.670783 0.062547  
C 3.039552 2.646009 7.300122 0.027039  
O 1.719408 4.554999 7.218918 -0.375643  
O 4.164631 1.880973 6.807731 -0.329524  
H 1.611563 5.474796 6.876709 0.328913  
H 2.145916 2.034946 7.097061 0.102416  
H 3.161232 2.762879 8.390944 0.109537  
H 4.992063 2.390880 6.957873 0.353953  
H 3.766456 4.666990 6.862728 0.067549



(a) Front view of CHOH-CH<sub>2</sub>OH



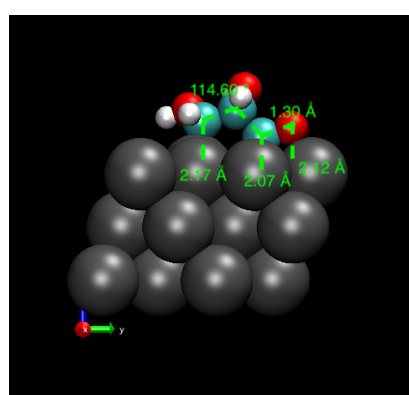
(b) Side view of CHOH-CH<sub>2</sub>OH



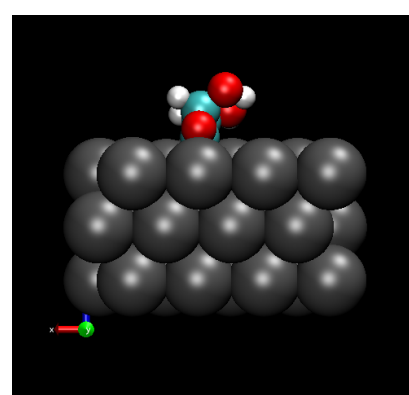
(c) Top view of CHOH-CH<sub>2</sub>OH

## 6.20 CO-CHOH-CHOH

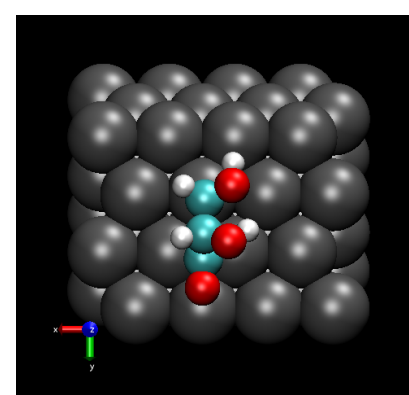
C 5.523577 4.234818 6.773776 0.049961  
C 5.552684 5.719915 7.257815 0.141601  
C 5.579031 6.775765 6.111088 0.108603  
O 4.355600 3.645251 7.273592 -0.393879  
O 4.500137 6.029922 8.136235 -0.428742  
O 5.621614 8.013294 6.494211 -0.189462  
H 4.312400 2.717486 6.947665 0.343811  
H 3.698154 5.569994 7.813092 0.359003  
H 6.494660 5.878611 7.811861 0.101583  
H 6.423800 3.683220 7.096455 0.082579



(a) Front view of CO-CHOH-CHOH



(b) Side view of CO-CHOH-CHOH

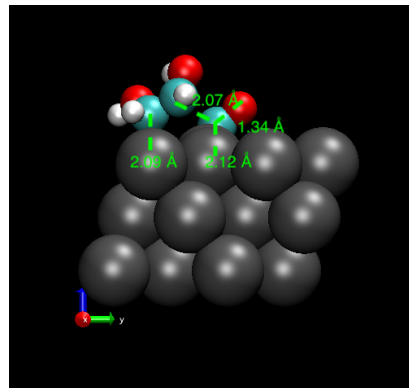


(c) Top view of CO-CHOH-CHOH

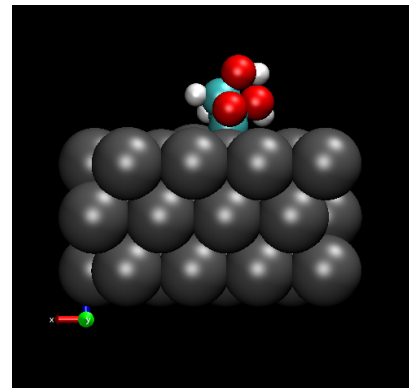
## 6.21 (CO)-CHOH-CHOH

C 4.161051 1.499295 6.649902 0.020610  
C 4.467002 2.750692 7.379390 0.178967

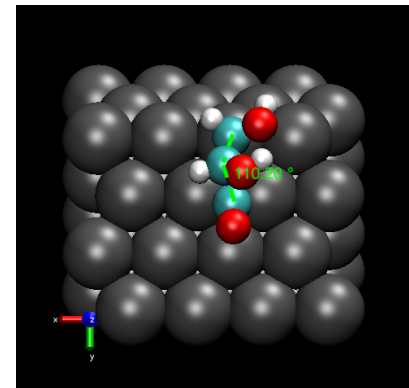
C 4.150032 4.385049 6.156785 0.088897  
 O 2.960433 1.002313 7.168379 -0.404357  
 O 3.721594 3.032293 8.455020 -0.328630  
 O 4.087767 5.346605 6.897812 -0.191521  
 H 2.693879 0.203671 6.635356 0.320336  
 H 2.887878 2.505447 8.383499 0.384247  
 H 5.518011 3.021856 7.495860 0.105149  
 H 5.007582 0.787524 6.772687 0.095465



(a) Front view of (CO)-CHOH-CHOH



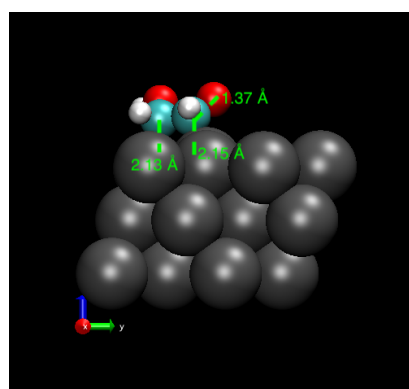
(b) Side view of (CO)-CHOH-CHOH



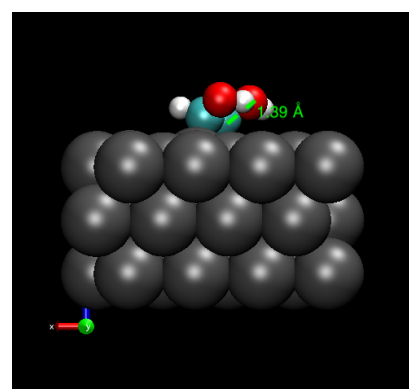
(c) Top view of (CO)-CHOH-CHOH

## 6.22 CHOH-CHOH

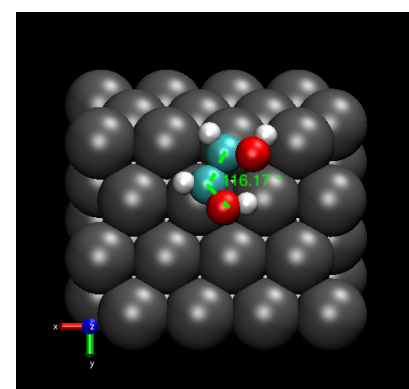
C 4.543977 2.037696 6.594703 0.064674  
 C 5.254117 3.373368 6.719445 0.106972  
 O 3.342304 2.065121 7.299718 -0.407448  
 O 4.593552 4.346323 7.426942 -0.362297  
 H 2.806493 1.287752 7.033025 0.353636  
 H 3.625678 4.182194 7.346303 0.362558  
 H 6.292739 3.294827 7.072770 0.104875  
 H 5.206967 1.197083 6.866561 0.088421



(a) Front view of CHOH-CHOH



(b) Side view of CHOH-CHOH



(c) Top view of CHOH-CHOH

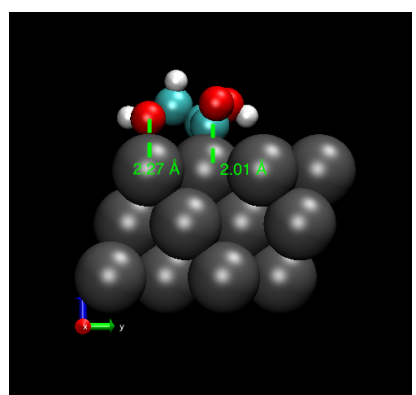
## 6.23 CO-COH-CH<sub>2</sub>OH

C 4.996776 4.249434 6.482570 0.210294  
 C 3.441093 4.006015 6.587077 0.142129  
 C 3.163902 2.684017 7.315213 0.007100  
 O 5.680423 4.536515 7.432531 -0.234290  
 O 2.804753 4.969534 7.358347 -0.392862  
 O 3.996990 1.614114 6.790138 -0.298813  
 H 2.099248 2.425166 7.195595 0.093449

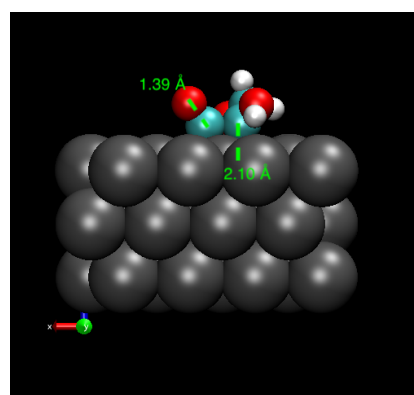
H 3.427752 2.808525 8.378355 0.124571

H 3.497075 0.767437 6.837328 0.345172

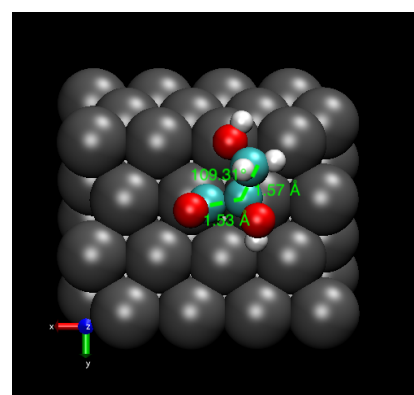
H 2.874009 5.832382 6.888955 0.328945



(a) Front view of CO-COH-CH<sub>2</sub>OH



(b) Side view of CO-COH-CH<sub>2</sub>OH



(c) Top view of CO-COH-CH<sub>2</sub>OH

## 6.24 (CO)-COH-CH<sub>2</sub>OH

C 5.231675 4.218763 6.483458 0.185679

C 3.198710 4.085791 6.546525 0.144083

C 3.054801 2.817815 7.368999 -0.006880

O 5.725767 4.382843 7.541899 -0.170066

O 2.783703 5.125062 7.296672 -0.337032

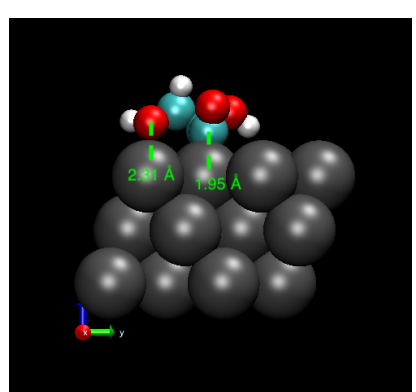
O 3.898481 1.752082 6.869608 -0.323971

H 1.993333 2.513134 7.305146 0.098548

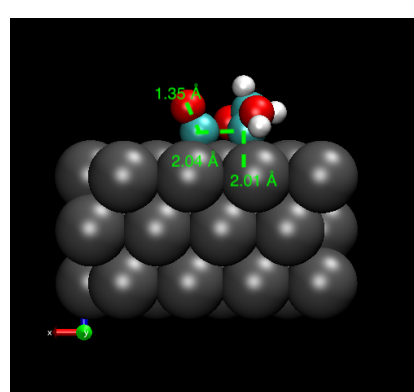
H 3.342506 3.032371 8.411381 0.124682

H 3.405601 0.906220 6.945546 0.347057

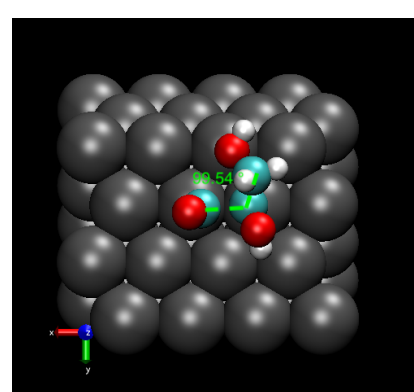
H 2.663886 5.917901 6.709438 0.322948



(a) Front view of (CO)-COH-CH<sub>2</sub>OH



(b) Side view of (CO)-COH-CH<sub>2</sub>OH



(c) Top view of (CO)-COH-CH<sub>2</sub>OH

## 6.25 COH-CH<sub>2</sub>OH

C 2.820283 4.066821 6.496249 0.218162

C 2.928521 2.848864 7.397244 -0.016791

O 2.673098 5.142797 7.233887 -0.284056

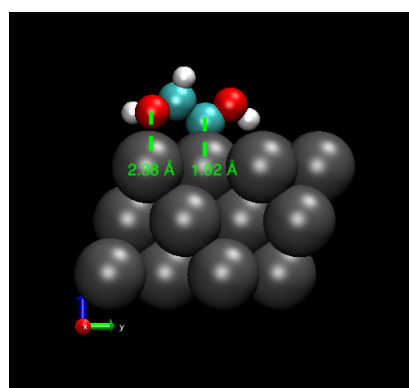
O 3.822078 1.825551 6.928337 -0.333895

H 1.895341 2.455195 7.452262 0.119265

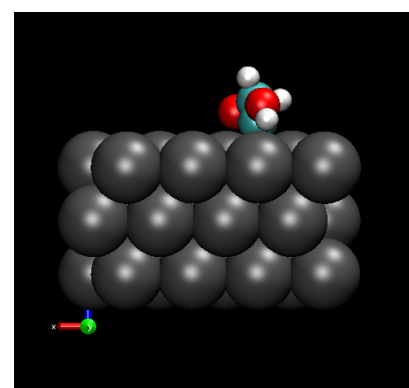
H 3.266428 3.165382 8.395403 0.128419

H 3.341788 0.967862 6.899911 0.338830

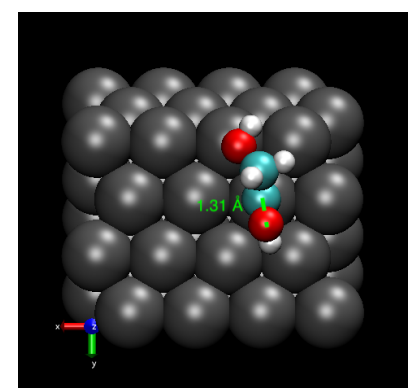
H 2.511876 5.931371 6.621576 0.315782



(a) Front view of COH-CH<sub>2</sub>OH



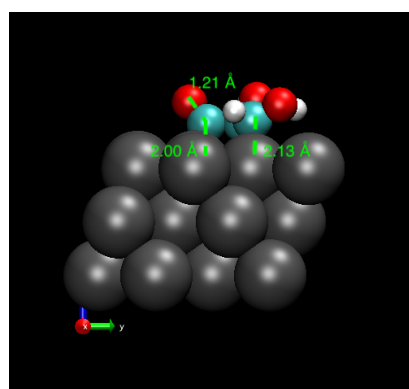
(b) Side view of COH-CH<sub>2</sub>OH



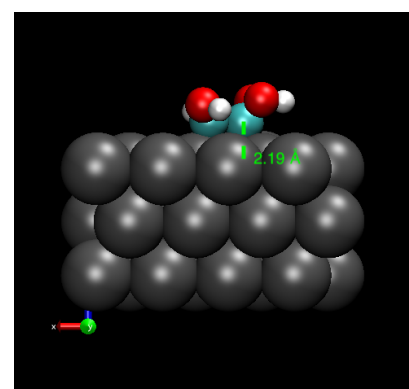
(c) Top view of COH-CH<sub>2</sub>OH

## 6.26 CHOH-COH-CO

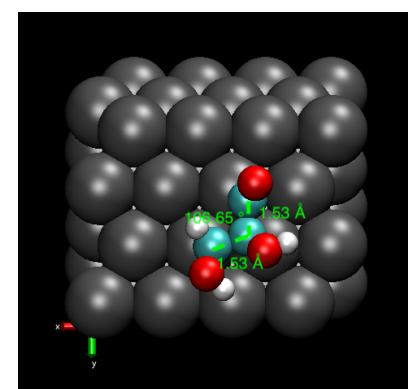
C 4.943008 4.698818 6.470142 0.201360  
 C 4.948394 6.231709 6.511824 0.131247  
 C 6.411409 6.662346 6.586532 0.074120  
 O 4.603408 3.969641 7.372429 -0.246949  
 O 4.185351 6.837719 7.485631 -0.394140  
 O 6.671577 7.826116 7.261527 -0.341674  
 H 7.075787 5.880779 6.986178 0.114817  
 H 3.262196 6.522231 7.397930 0.376026  
 H 5.966657 8.487868 7.064760 0.349925



(a) Front view of CHOH-COH-CO



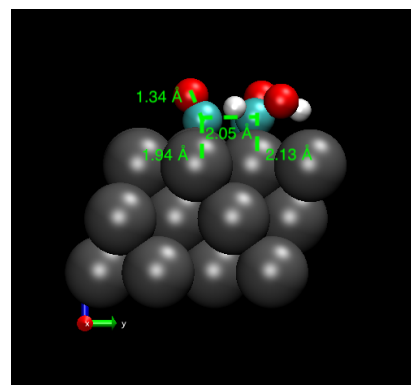
(b) Side view of CHOH-COH-CO



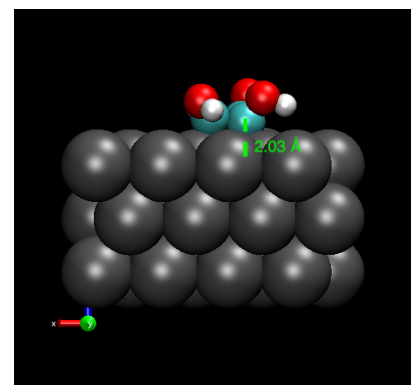
(c) Top view of CHOH-COH-CO

## 6.27 CHOH-COH-(CO)

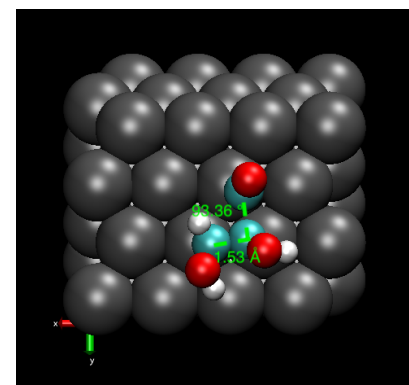
C 4.943008 4.698818 6.470142 0.201360  
 C 4.948394 6.231709 6.511824 0.131247  
 C 6.411409 6.662346 6.586532 0.074120  
 O 4.603408 3.969641 7.372429 -0.246949  
 O 4.185351 6.837719 7.485631 -0.394140  
 O 6.671577 7.826116 7.261527 -0.341674  
 H 7.075787 5.880779 6.986178 0.114817  
 H 3.262196 6.522231 7.397930 0.376026  
 H 5.966657 8.487868 7.064760 0.349925



(a) Front view of CHOH-COH-(CO)



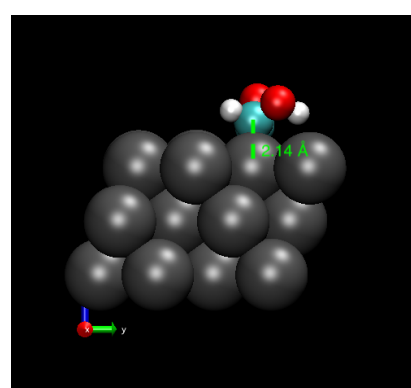
(b) Side view of CHOH-COH-(CO)



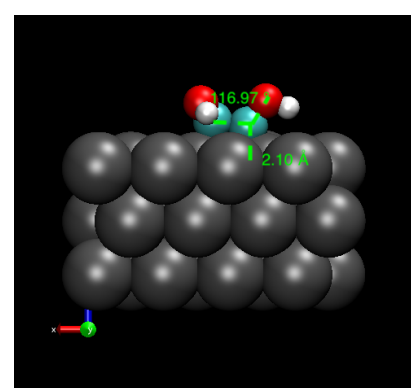
(c) Top view of CHOH-COH-(CO)

## 6.28 CHOH-COH

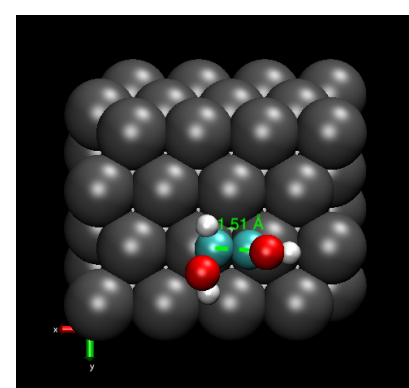
C 4.823304 6.892441 6.313605 0.195571  
C 6.297730 6.699158 6.549592 0.038256  
O 4.085339 7.172769 7.362866 -0.270993  
O 6.911569 7.655991 7.339544 -0.346373  
H 6.508055 5.703842 6.974073 0.128555  
H 3.145084 7.290193 7.066293 0.364942  
H 6.726772 8.540336 6.944961 0.323606



(a) Front view of CHOH-COH-(CO)



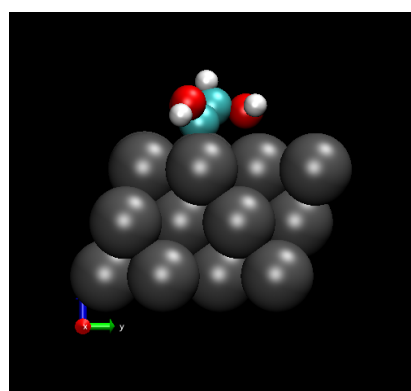
(b) Side view of CHOH-COH-(CO)



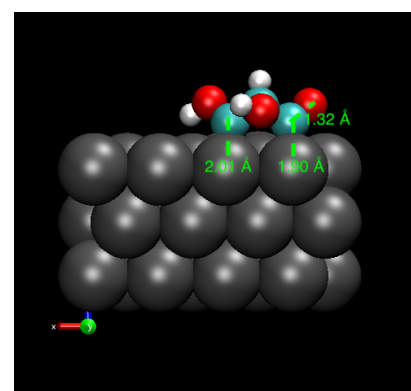
(c) Top view of CHOH-COH-(CO)

## 6.29 COH-CHOH-CO

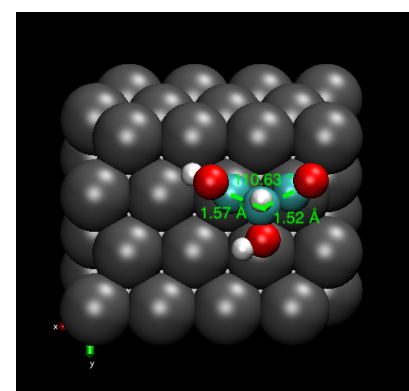
C 2.854810 4.067444 6.540271 0.247278  
C 4.149365 4.657837 7.202999 0.085842  
C 5.391171 4.114363 6.525946 0.174994  
O 2.010942 3.572425 7.252973 -0.265391  
O 4.062661 6.082196 7.016623 -0.377241  
O 6.274851 3.631472 7.372913 -0.290531  
H 7.063040 3.304429 6.852721 0.347144  
H 4.136237 4.407324 8.277621 0.111914  
H 4.919781 6.487887 7.265522 0.362295



(a) Front view of CHOH-CHOH-CO



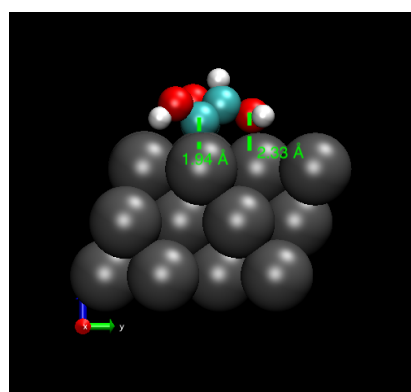
(b) Side view of CHOH-CHOH-CO



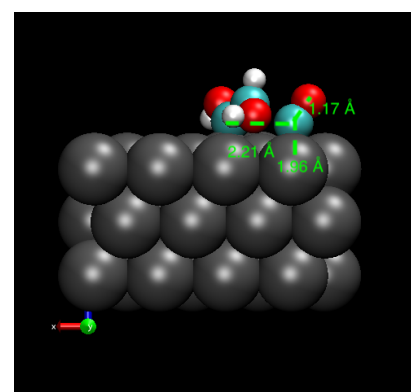
(c) Top view of CHOH-CHOH-CO

### 6.30 COH-CHOH-(CO)

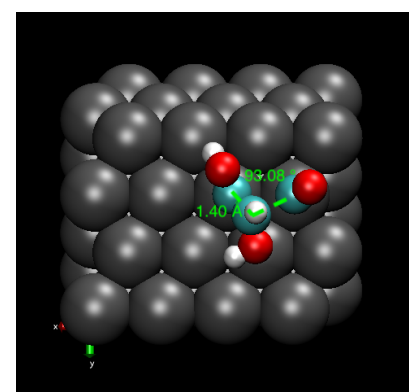
C 2.854810 4.067444 6.540271 0.247278  
C 4.149365 4.657837 7.202999 0.085842  
C 5.391171 4.114363 6.525946 0.174994  
O 2.010942 3.572425 7.252973 -0.265391  
O 4.062661 6.082196 7.016623 -0.377241  
O 6.274851 3.631472 7.372913 -0.290531  
H 7.063040 3.304429 6.852721 0.347144  
H 4.136237 4.407324 8.277621 0.111914  
H 4.919781 6.487887 7.265522 0.362295



(a) Front view of CHOH-CHOH-(CO)



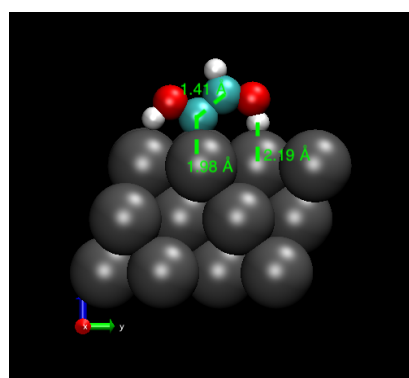
(b) Side view of CHOH-CHOH-(CO)



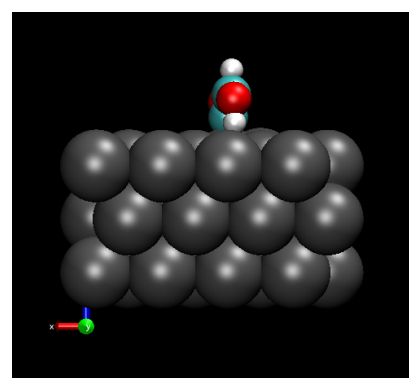
(c) Top view of CHOH-CHOH-(CO)

### 6.31 COH-CHOH

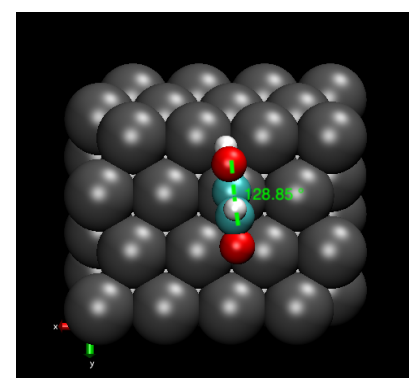
C 5.391485 5.071468 7.578416 0.157974  
C 5.578044 4.062468 6.613526 0.071800  
O 5.192640 6.354031 7.403922 -0.257777  
O 5.725352 2.873209 7.235017 -0.308268  
H 5.961597 2.170698 6.559679 0.302161  
H 5.414926 4.770353 8.631611 0.124204  
H 5.105184 6.586050 6.406551 0.254648



(a) Front view of CHOH-CHOH



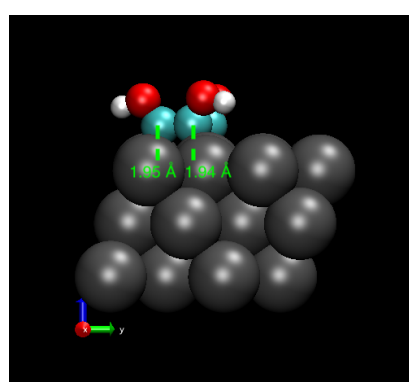
(b) Side view of CHOH-CHOH



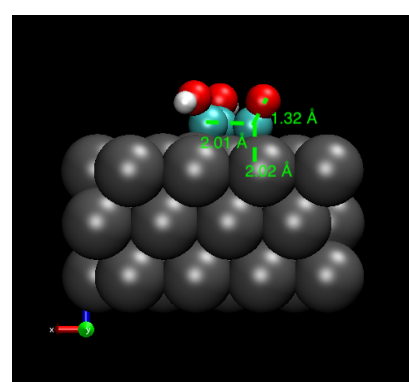
(c) Top view of CHOH-CHOH

### 6.32 COH-COH-(CO)

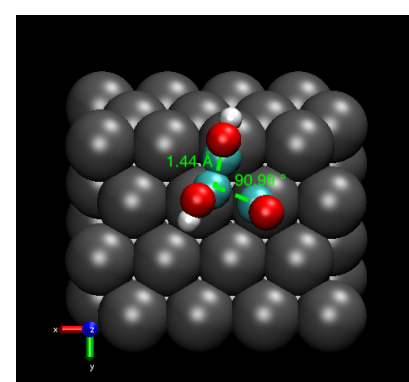
C 4.717218 2.137161 6.448299 0.151402  
 C 5.142143 3.509101 6.523810 0.080285  
 C 3.235728 4.139853 6.452225 0.183490  
 O 4.629896 1.382309 7.531268 -0.279895  
 O 5.736001 3.968144 7.647136 -0.339901  
 O 2.798402 4.492211 7.489084 -0.176162  
 H 4.328277 0.485389 7.257644 0.370086  
 H 6.122472 4.846532 7.451785 0.373273



(a) Front view of COH-COH-(CO)



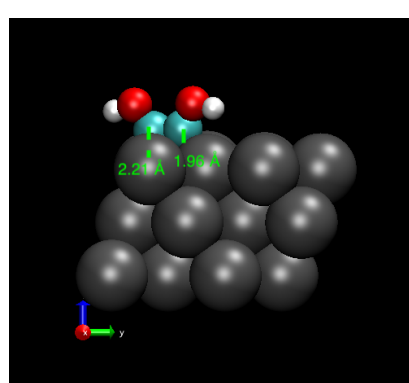
(b) Side view of COH-COH-(CO)



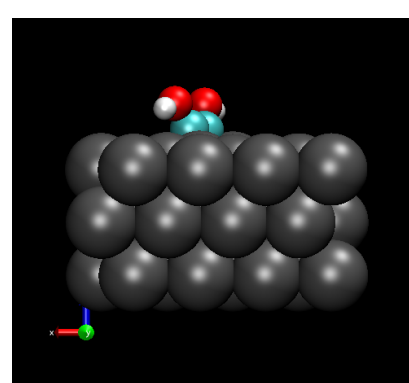
(c) Top view of COH-COH-(CO)

### 6.33 COH-COH

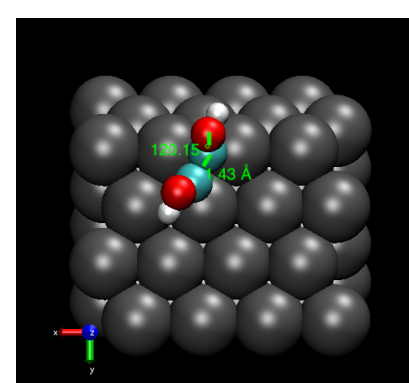
C 5.489735 1.752257 6.202067 0.113393  
 C 6.111510 3.035500 6.258769 0.140180  
 O 5.458956 0.969048 7.290263 -0.307570  
 O 6.724633 3.466953 7.360410 -0.299807  
 H 5.064764 0.104188 7.030951 0.354007  
 H 7.158132 4.325419 7.148578 0.364265



(a) Front view of COH-COH



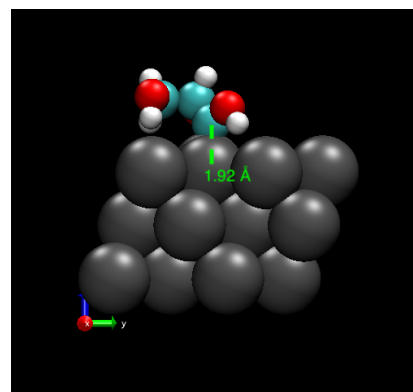
(b) Side view of COH-COH



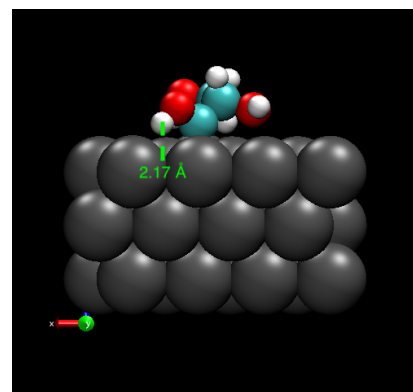
(c) Top view of COH-COH

### 6.34 COH-CHOH-CH<sub>2</sub>OH

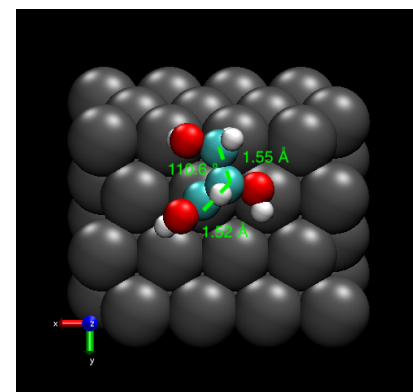
C 5.642452 4.159182 6.626116 0.201899  
C 4.667756 3.488430 7.582854 0.107038  
C 4.915671 1.963635 7.631496 0.049885  
O 6.547578 4.837309 7.285112 -0.274346  
O 3.303300 3.681393 7.206470 -0.418783  
O 6.266628 1.612482 7.781941 -0.425973  
H 7.188406 5.262359 6.630675 0.320422  
H 4.474666 1.532570 6.687609 0.044396  
H 4.347050 1.554552 8.479815 0.101721  
H 6.680165 1.564193 6.882116 0.282083  
H 4.852520 3.911351 8.586419 0.092761  
H 3.070836 4.622190 7.334440 0.357801



(a) Front view of COH-CHOH-CH<sub>2</sub>OH



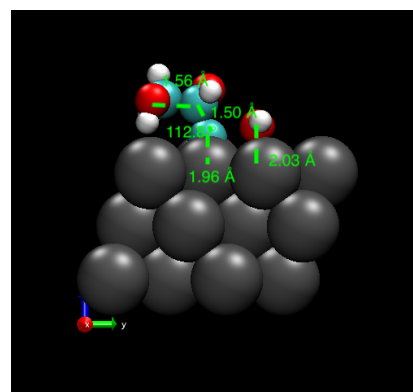
(b) Side view of COH-CHOH-CH<sub>2</sub>OH



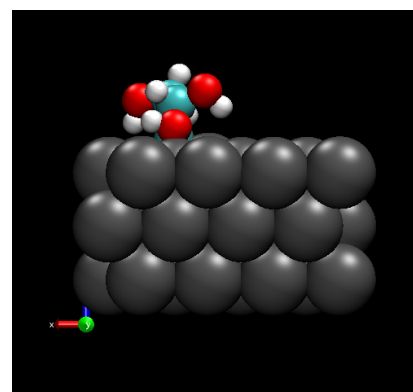
(c) Top view of COH-CHOH-CH<sub>2</sub>OH

### 6.35 C(OH)-CHOH-CH<sub>2</sub>OH

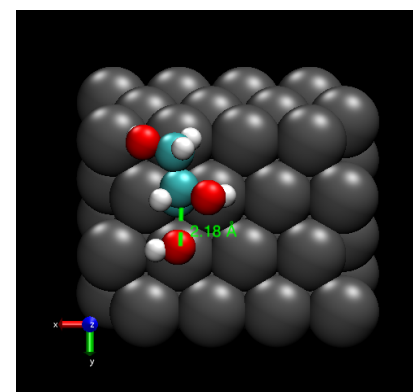
C 7.086161 4.031885 6.013603 -0.031526  
C 7.006122 3.644036 7.455873 0.158715  
C 7.210848 2.109202 7.682438 0.018479  
O 7.067242 6.154896 6.496471 -0.447383  
O 5.774096 4.040165 8.037760 -0.436239  
O 8.549260 1.686320 7.624496 -0.418806  
H 8.011013 6.290434 6.740367 0.333125  
H 6.544503 1.546545 6.991707 0.042202  
H 6.854426 1.944121 8.714026 0.111022  
H 8.775631 1.461861 6.688759 0.264725  
H 7.815477 4.151446 8.008829 0.105161  
H 5.071811 3.961633 7.354574 0.320414



(a) Front view of C(OH)-CHOH-CH<sub>2</sub>OH



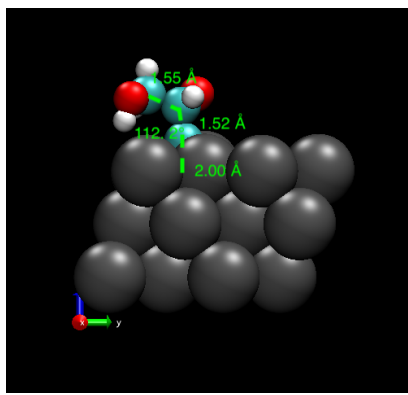
(b) Side view of C(OH)-CHOH-CH<sub>2</sub>OH



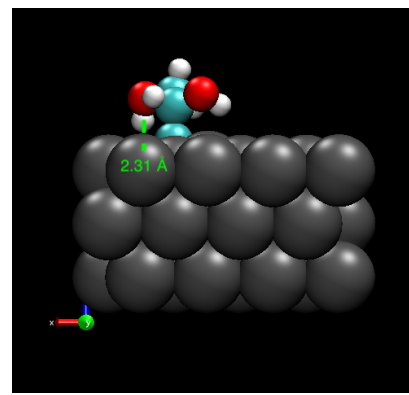
(c) Top view of C(OH)-CHOH-CH<sub>2</sub>OH

### 6.36 C-CHOH-CH<sub>2</sub>OH

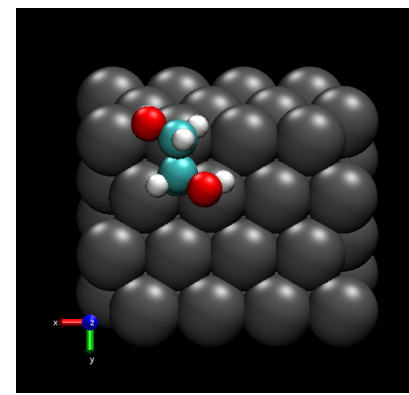
C 7.074850 3.146655 5.779472 -0.153585  
C 7.034387 3.033644 7.292133 0.181775  
C 7.040952 1.556156 7.770442 0.010714  
O 5.897032 3.704619 7.818962 -0.422900  
O 8.287239 0.904559 7.621772 -0.425692  
H 7.305844 7.434194 6.750958 0.341040  
H 6.224325 1.020379 7.242664 0.039704  
H 8.385995 0.619761 6.683513 0.260733  
H 7.923647 3.543260 7.697731 0.109643  
H 5.102141 3.380229 7.344063 0.321368



(a) Front view of C-CHOH-CH<sub>2</sub>OH



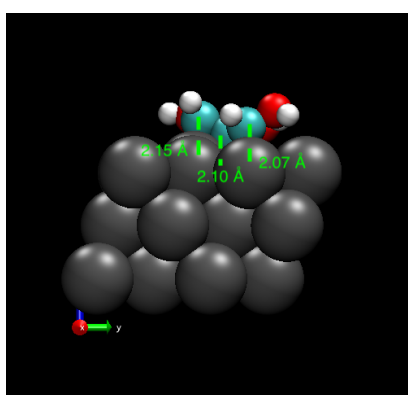
(b) Side view of C-CHOH-CH<sub>2</sub>OH



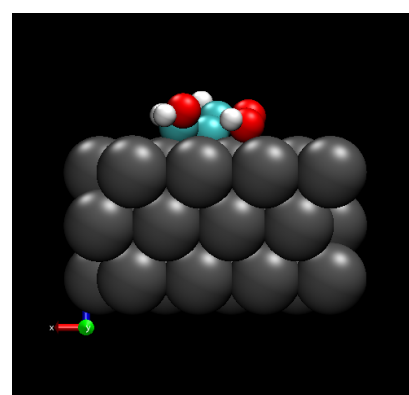
(c) Top view of C-CHOH-CH<sub>2</sub>OH

### 6.37 CHOH-C(OH)-CHOH

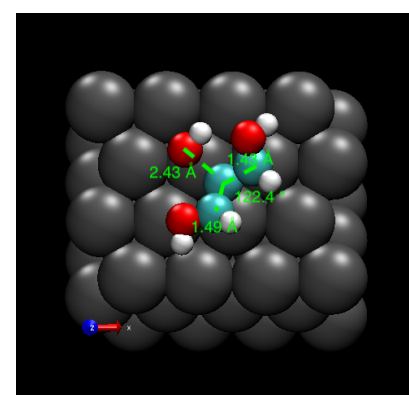
C 6.522993 6.318131 6.472786 0.076964  
C 5.273821 5.619109 6.073361 0.022121  
C 4.969352 4.316382 6.569303 0.092172  
O 6.320365 7.518012 7.173302 -0.401282  
O 3.656401 7.039338 6.517695 -0.466638  
O 3.634396 3.974966 6.776843 -0.280656  
H 7.253263 5.656845 6.971350 0.092382  
H 7.083434 8.104100 6.976152 0.348514  
H 4.316506 7.726144 6.779829 0.336829  
H 5.663480 3.855434 7.281581 0.113109  
H 3.576463 2.994490 6.876043 0.352494



(a) Front view of CHOH-C(OH)-CHOH



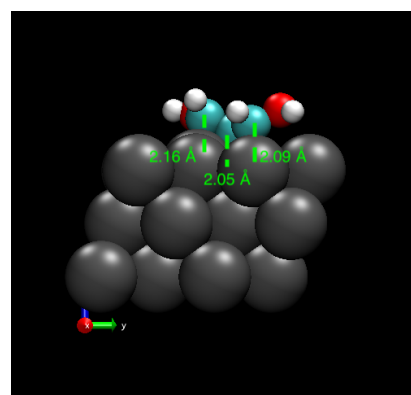
(b) Side view of CHOH-C(OH)-CHOH



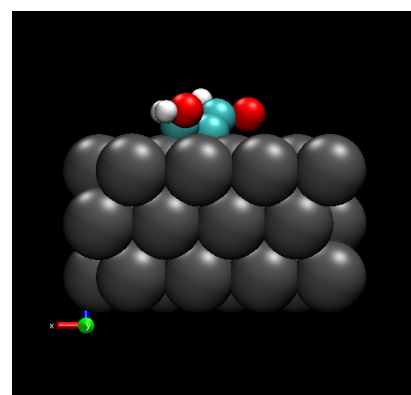
(c) Top view of CHOH-C(OH)-CHOH

### 6.38 CHOH-C-CHOH

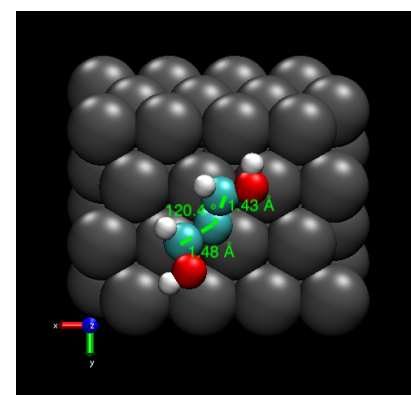
C 6.422038 6.413407 6.495866 0.088270  
C 5.165674 5.698030 6.155937 -0.061438  
C 4.857771 4.441618 6.770710 0.118222  
O 6.174627 7.656883 7.101782 -0.379939  
O 2.927376 8.972138 6.544528 -0.539136  
H 7.178633 5.822412 7.039219 0.086024  
H 7.004237 8.179755 7.047511 0.350025  
H 5.520761 4.027113 7.540104 0.107325  
H 3.479312 3.103769 7.090100 0.371001



(a) Front view of CHOH-C(OH)-CHOH



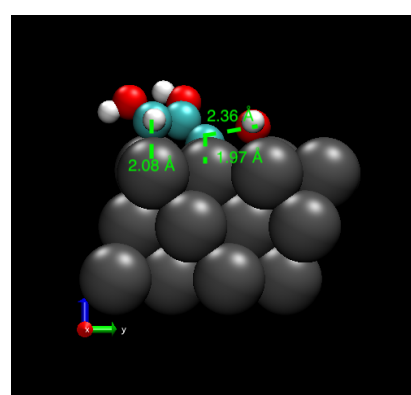
(b) Side view of CHOH-C(OH)-CHOH



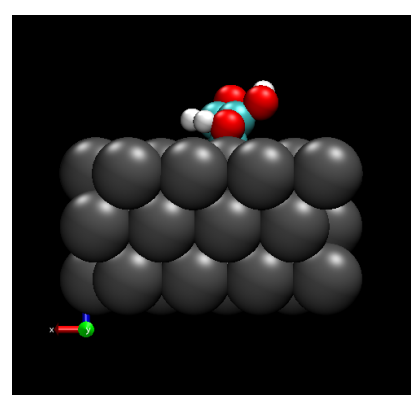
(c) Top view of CHOH-C(OH)-CHOH

### 6.39 C(OH)-COH-CHOH

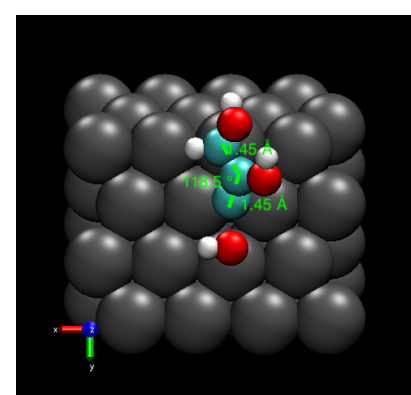
C 5.965862 1.715153 6.776411 0.012170  
C 5.211960 2.955909 6.797913 0.321119  
C 5.518370 3.966142 5.806457 -0.117303  
O 5.389879 0.739604 7.580893 -0.425408  
O 4.121857 3.051214 7.554368 -0.346741  
O 5.553952 6.019008 6.528695 -0.466730  
H 5.549913 9.582987 7.166862 0.366345  
H 4.016032 2.186976 8.018322 0.392828  
H 6.510167 6.020009 6.756004 0.329774  
H 7.059332 1.792966 6.829255 0.108307



(a) Front view of C(OH)-COH-CHOH



(b) Side view of C(OH)-COH-CHOH

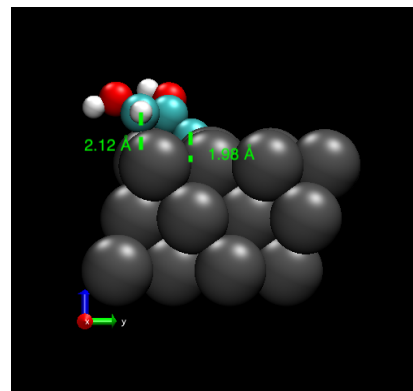


(c) Top view of C(OH)-COH-CHOH

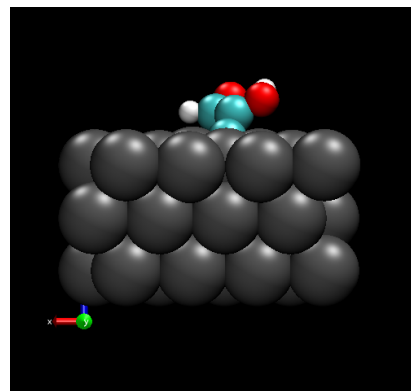
### 6.40 C-COH-CHOH

C 5.950781 1.105606 6.781455 0.052683  
C 5.162364 2.327383 6.732766 0.313334

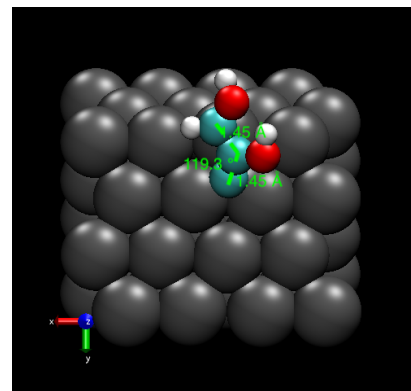
C 5.455937 3.321241 5.718711 -0.207153  
 O 5.318077 0.071476 7.385154 -0.409671  
 O 3.980181 2.348140 7.361711 -0.363251  
 H 5.580389 8.840370 7.046337 0.367568  
 H 3.855068 1.454495 7.766794 0.387095  
 H 7.045530 1.150795 6.827428 0.108653



(a) Front view of C-COH-CHOH



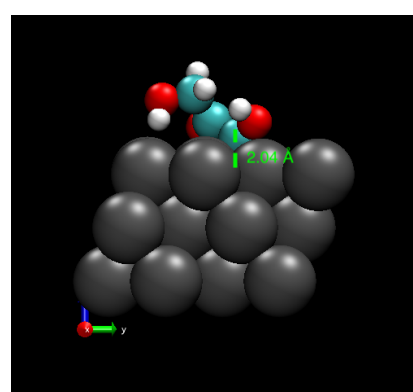
(b) Side view of C-COH-CHOH



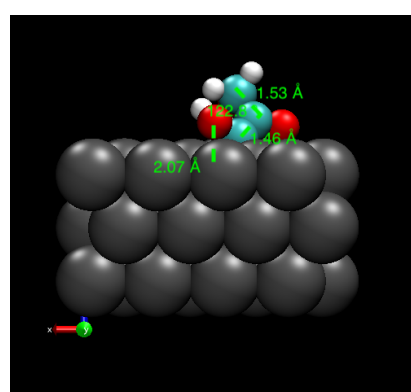
(c) Top view of C-COH-CHOH

#### 6.41 COH-CO-CH<sub>2</sub>OH

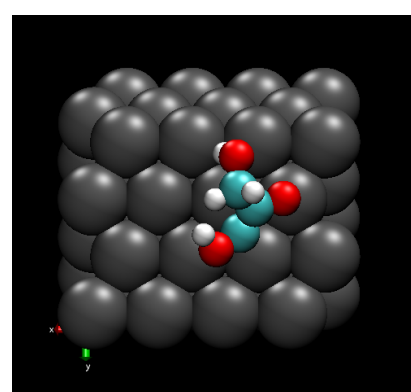
C 4.915394 3.826426 8.023315 -0.005918  
 C 4.258848 4.560705 6.861578 0.262930  
 C 4.930060 5.618508 6.112621 0.032227  
 O 5.010323 2.437285 7.778471 -0.403436  
 O 3.057830 4.193429 6.583324 -0.248113  
 O 5.966646 6.305829 6.770649 -0.323498  
 H 5.531152 2.302582 6.951215 0.283225  
 H 6.545476 5.668527 7.248655 0.353824  
 H 5.905515 4.263934 8.265092 0.059002  
 H 4.272201 3.948485 8.910268 0.128918



(a) Front view of COH-CO-CH<sub>2</sub>OH



(b) Side view of COH-CO-CH<sub>2</sub>OH



(c) Top view of COH-CO-CH<sub>2</sub>OH

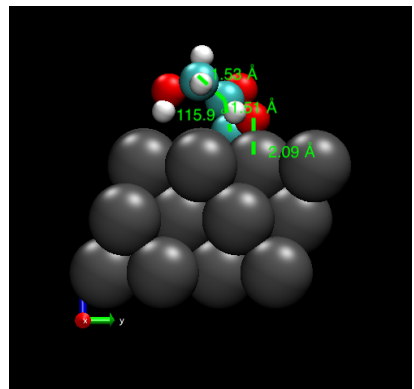
#### 6.42 C(OH)-CO-CH<sub>2</sub>OH

C 4.958976 4.111545 8.151950 -0.023961  
 C 4.259588 5.210893 7.350075 0.404340  
 C 4.766874 5.430298 5.939056 -0.088154  
 O 4.505180 2.828807 7.747079 -0.409396  
 O 3.314845 5.861441 7.768646 -0.318473  
 O 6.434737 6.389890 6.537043 -0.418808  
 H 4.918199 2.605009 6.878262 0.275326

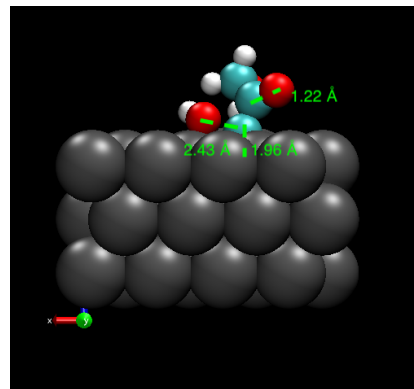
H 7.016260 5.651238 6.831658 0.330276

H 6.059264 4.206383 8.045790 0.067910

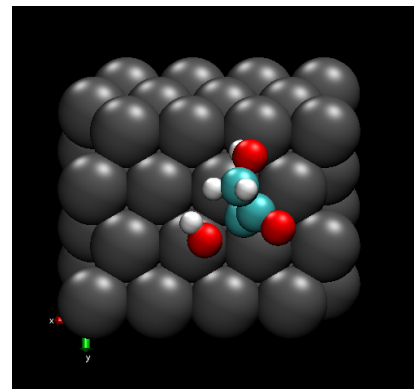
H 4.677185 4.238016 9.204843 0.123111



(a) Front view of C(OH)-CO-CH<sub>2</sub>OH



(b) Side view of C(OH)-CO-CH<sub>2</sub>OH



(c) Top view of C(OH)-CO-CH<sub>2</sub>OH

#### 6.43 C-CO-CH<sub>2</sub>OH

C 6.928782 3.646758 7.880395 -0.033197

C 7.256556 4.985647 7.212078 0.430030

C 7.017091 5.038582 5.736640 -0.249199

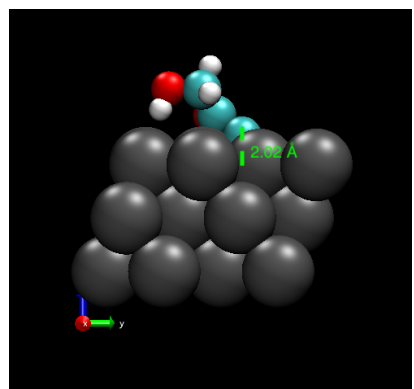
O 5.541913 3.354399 7.783817 -0.402544

O 7.712551 5.964491 7.794268 -0.340530

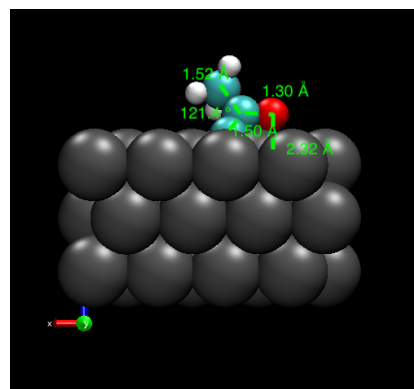
H 5.375327 2.885347 6.935620 0.284431

H 7.547996 2.866066 7.395206 0.082652

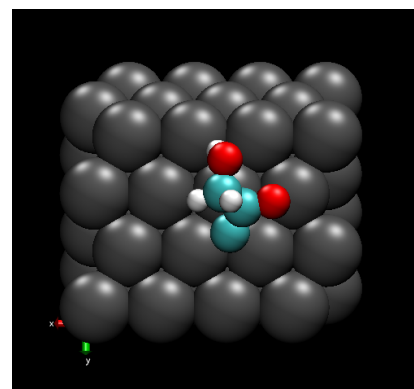
H 7.186919 3.724192 8.946644 0.118829



(a) Front view of C-CO-CH<sub>2</sub>OH



(b) Side view of C-CO-CH<sub>2</sub>OH



(c) Top view of C-CO-CH<sub>2</sub>OH

#### 6.44 C(OH)-COH-COH

C 4.495739 1.928990 6.610141 0.144758

C 5.165247 3.053945 7.281406 0.188696

C 5.675845 3.992633 6.417963 -0.076024

O 4.015909 1.034800 7.462217 -0.276578

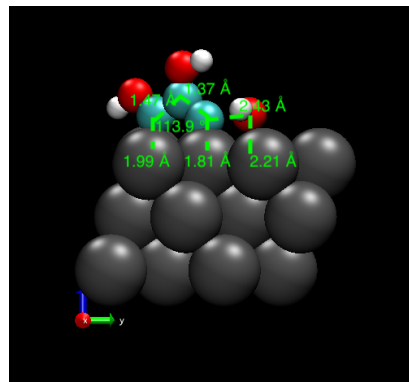
O 5.209032 3.052818 8.644025 -0.382918

O 6.770920 5.914481 6.649152 -0.485200

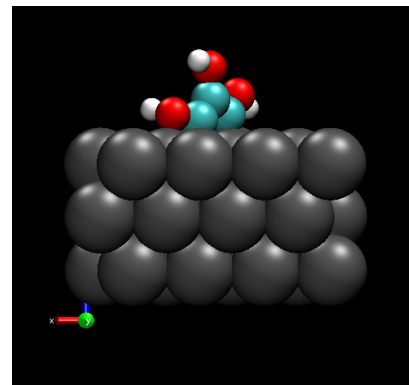
H 7.660819 5.554785 6.873881 0.327337

H 3.591039 0.306877 6.941334 0.347725

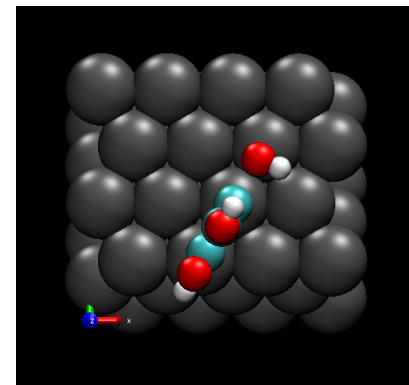
H 5.651597 3.867076 8.944014 0.386050



(a) Front view of C(OH)-COH-COH



(b) Side view of C(OH)-COH-COH



(c) Top view of C(OH)-COH-COH

## 6.45 C-COH-COH

C 4.322117 1.641996 6.610917 0.146757

C 5.008749 2.716096 7.269263 0.214823

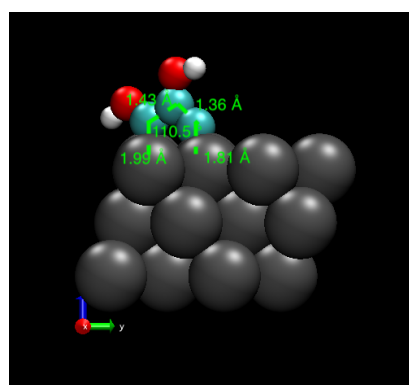
C 5.473262 3.618021 6.355828 -0.136166

O 3.769003 0.718875 7.367691 -0.260283

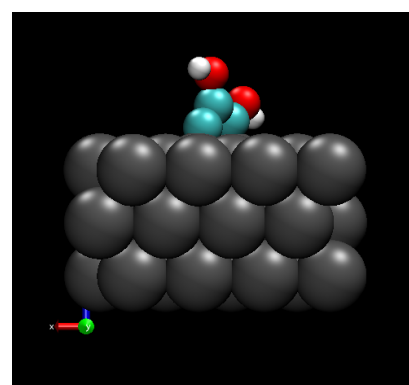
O 5.118041 2.771674 8.625695 -0.384999

H 3.338466 0.040913 6.760341 0.314934

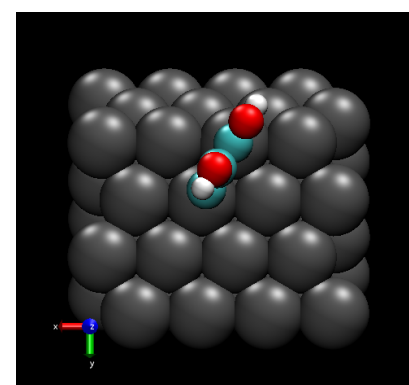
H 5.628156 3.569120 8.871105 0.385760



(a) Front view of C-COH-COH



(b) Side view of C-COH-COH



(c) Top view of C-COH-COH

## 7 Parameters and Reaction Energetics of Microkinetic Modeling

### 7.1 Adsorption Parameters

Desorption rate constants were calculated as<sup>37-39</sup>,

$$k = \frac{k_B T^3}{h^3} \frac{A(2\pi m k_B)}{\sigma \theta} \exp\left(\frac{-E_{\text{des}}}{k_B T}\right) \quad (13)$$

where  $h$  is the Plank's constant,  $\sigma$  is the symmetry number,  $\theta$  is the rotational temperature of the species, and  $E_{\text{des}}$  is the desorption energy. Note that this equation only applies to saturated chemical species, which are CH<sub>2</sub>OH-CHOH-CH<sub>2</sub>OH, CO, CO<sub>2</sub>, H<sub>2</sub>, H<sub>2</sub>O, CH<sub>2</sub>OH-CH<sub>2</sub>OH, and CH<sub>3</sub>OH. Detailed symmetry numbers and rotational temperature of those species can be obtained from either NIST webbook<sup>40</sup> or from calculations done in Gaussian 09<sup>41</sup>. Table 7 lists the  $\sigma$  and  $\theta$  used for those adsorbing/desorbing species.

Table 7: Adsorption parameters for species studied in MKM.

| Chemical species                           | $\sigma$ | $\theta/K$ |
|--|----------|------------|
| CH <sub>2</sub> OH-CHOH-CH <sub>2</sub> OH | 1        | 0.192      |
| CO   | 1        | 2.770      |
| CO <sub>2</sub>                            | 2        | 0.534      |
| H <sub>2</sub>                             | 2        | 87.150     |
| H <sub>2</sub> O                           | 2        | 39.370     |
| CH <sub>2</sub> OH-CH <sub>2</sub> OH      | 1        | 0.636      |
| CH <sub>3</sub> OH                         | 1        | 5.930      |

## 7.2 Reaction Energetics of Microkinetic Modeling in Vacuum and Aqueous Phases

The table below include the reactions and their energies used in the microkinetic modeling in addition to the reactions explicitly calculated and estimated from transition state scaling relations in this work.

Table 8: Reaction energies and activation energies of reactions included in the microkinetic model, in addition to those tabulated in Table 1 in the main manuscript text. Energy unit in eV. Identifier: a, adsorption and desorption reactions; d, direct reactions; w, water gas shift reactions; c, methanation reactions; e, reactions related to C<sub>2</sub> species and their derivatives; m: water mediated reactions. For each identifier (d, w, c, e, m), the source of the energetics is provided in the first entry. For reactions where aqueous phase data is not available, the vacuum energies are used in both microkinetic models.

| Identifier      | Reaction  | $E_{\text{rxn}}^{\text{vac}}$ | $E_{\text{rxn}}^{\text{aq}}$ | $E_{\text{act}}^{\text{vac}}$ | $E_{\text{act}}^{\text{aq}}$ |
|-----------------|---|-------------------------------|------------------------------|-------------------------------|------------------------------|
| a[This work]    | CH <sub>2</sub> OH-CHOH-CH <sub>2</sub> OH + * → CH <sub>2</sub> OH-CHOH-CH <sub>2</sub> OH*      | -0.65                         | -1.06                        | N/A                           | N/A                          |
| a               | CO <sub>2</sub> + * → CO <sub>2</sub> *   | -0.17                         | -0.17                        | N/A                           | N/A                          |
| a               | H <sub>2</sub> O + * → H <sub>2</sub> O*  | -0.41                         | -0.41                        | N/A                           | N/A                          |
| a               | CH <sub>3</sub> -CH <sub>3</sub> + * → CH <sub>3</sub> -CH <sub>3</sub> *                         | -0.55                         | -0.55                        | N/A                           | N/A                          |
| a <sup>42</sup> | CH <sub>2</sub> OH-CH <sub>2</sub> OH + * → CH <sub>2</sub> OH-CH <sub>2</sub> OH*                | -0.46                         | -0.46                        | N/A                           | N/A                          |
| a <sup>42</sup> | CH <sub>3</sub> OH + * → CH <sub>3</sub> OH*  | -0.27                         | -0.27                        | N/A                           | N/A                          |
| a <sup>42</sup> | H <sub>2</sub> + 2* → 2H*   | -0.96                         | -0.96                        | N/A                           | N/A                          |
| a <sup>42</sup> | CO + * → CO*  | -1.79                         | -1.79                        | N/A                           | N/A                          |
| d[This work]    | CH <sub>2</sub> OH-CHOH-CH <sub>2</sub> OH* + * → CH <sub>2</sub> OH-COH-CH <sub>2</sub> OH* + H* | -0.45                         | -0.44                        | 0.36                          | 0.30                         |
| d               | CH <sub>2</sub> OH-CHOH-CH <sub>2</sub> OH* + * → CHO <sub>2</sub> -CHOH-CH <sub>2</sub> OH* + H* | -0.46                         | -0.27                        | 0.60                          | 0.83                         |
| d               | CH <sub>2</sub> OH-CHOH-CH <sub>2</sub> OH* + * → CH <sub>2</sub> O-CHOH-CH <sub>2</sub> OH* + H* | -0.30                         | 0.43                         | 0.66                          | 1.28                         |
| d               | CH <sub>2</sub> OH-CHOH-CH <sub>2</sub> OH* + * → CH <sub>2</sub> OH-CHO-CH <sub>2</sub> OH* + H* | -0.29                         | 0.40                         | 1.24                          | 0.65                         |
| d               | CHOH-CHOH-CH <sub>2</sub> OH* + * → COH-CHOH-CH <sub>2</sub> OH* + H*                             | -0.17                         | -0.34                        | 0.39                          | 0.57                         |
| d               | CHOH-CHOH-CH <sub>2</sub> OH* + * → CHO <sub>2</sub> -CHOH-CHOH* + H*                             | -0.15                         | -0.18                        | 0.47                          | 0.55                         |
| d               | CHOH-CHOH-CH <sub>2</sub> OH* + * → CHO-CHOH-CH <sub>2</sub> OH* + H*                             | 0.02                          | -0.22                        | 0.69                          | 0.52                         |
| d               | CH <sub>2</sub> O-CHOH-CH <sub>2</sub> OH* + * → CHO-CHOH-CH <sub>2</sub> OH* + H*                | -0.35                         | -0.21                        | 0.66                          | 0.51                         |
| d               | CH <sub>2</sub> OH-COH-CH <sub>2</sub> OH* + * → CH <sub>2</sub> OH-CO-CH <sub>2</sub> OH* + H*   | 0.55                          | 0.31                         | 1.24                          | 0.70                         |
| d               | CH <sub>2</sub> OH-CHO-CH <sub>2</sub> OH* + * → CH <sub>2</sub> OH-CO-CH <sub>2</sub> OH* + H*   | -0.37                         | -0.25                        | 0.73                          | 0.60                         |
| d               | CH <sub>2</sub> OH-COH-CH <sub>2</sub> OH* + * → CHO <sub>2</sub> -COH-CH <sub>2</sub> OH* + H*   | -0.35                         | -0.39                        | 0.60                          | 0.48                         |
| d               | CHOH-COH-CH <sub>2</sub> OH* + * → CHO <sub>2</sub> -COH-CHOH* + H*                               | -0.08                         | -0.10                        | 1.01                          | 1.09                         |
| d               | CHOH-CHOH-CHOH* + * → CHO <sub>2</sub> -COH-CHOH* + H*  | -0.34                         | -0.29                        | 0.77                          | 0.57                         |
| d               | CHOH-COH-CHOH* + * → COH-COH-CHOH* + H*   | -0.19                         | -0.11                        | 0.38                          | 0.35                         |
| d               | COH-COH-CHOH* + * → COH-COH-COH* + H*   | -0.33                         | -0.38                        | 0.47                          | 0.45                         |
| d               | COH-COH-COH* + * → COH-COH-CO* + H*   | 0.20                          | 0.24                         | 0.40                          | 0.38                         |
| d               | COH-COH-CO* + * → CO-COH-CO* + H*   | 0.26                          | 0.26                         | 0.67                          | 0.66                         |

|                 |   |       |       |       |      |
|-----------------|---|-------|-------|-------|------|
| d               | $\text{CHO-CHOH-CH}_2\text{OH}^* + * \rightarrow \text{CO-CHOH-CH}_2\text{OH}^* + \text{H}^*$                   | -0.23 | -0.19 | 0.36  | 0.46 |
| d               | $\text{CO-CHOH-CH}_2\text{OH}^* + * \rightarrow \text{CO-CHOH-CHOH}^* + \text{H}^*$                             | -0.40 | -0.20 | 0.20  | 0.48 |
| d               | $\text{CH}_2\text{O-COH-CH}_2\text{OH}^* + * \rightarrow \text{CH}_2\text{O-CO-CH}_2\text{OH}^* + \text{H}^*$   | 0.55  | 0.20  | 0.69  | 0.60 |
| d               | $\text{CHOH-CHOH-CHOH}^* + * \rightarrow \text{CHOH-COH-CHOH}^* + \text{H}^*$                                   | -0.28 | -0.18 | 0.72  | 0.57 |
| d               | $\text{CH}_2\text{OH-CHO-CH}_2\text{OH}^* + * \rightarrow \text{CH}_2\text{OH-CO-CH}_2\text{OH}^* + \text{H}^*$ | 0.47  | 0.25  | 0.73  | 0.59 |
| d               | $\text{CO-CHOH-CH}_2\text{OH}^* + * \rightarrow \text{CHOH-CH}_2\text{OH}^* + \text{CO}^*$                      | -0.94 | 0.52  | 1.08  | 0.90 |
| d               | $\text{CO-CHOH-CHOH}^* + * \rightarrow \text{CHOH-CHOH}^* + \text{CO}^*$  | -1.17 | -1.03 | 0.56  | 0.60 |
| d               | $\text{CO-COH-CH}_2\text{OH}^* + * \rightarrow \text{COH-CH}_2\text{OH}^* + \text{CO}^*$                        | -0.61 | -0.34 | 0.30  | 0.43 |
| d               | $\text{CO-COH-CHOH}^* + * \rightarrow \text{COH-CHOH}^* + \text{CO}^*$  | -0.61 | -0.55 | 0.46  | 0.72 |
| d               | $\text{CO-CHOH-COH}^* + * \rightarrow \text{COH-CHOH}^* + \text{CO}^*$  | -0.34 | 0.15  | 0.37  | 0.70 |
| d               | $\text{CO-COH-COH}^* + * \rightarrow \text{COH-COH}^* + \text{CO}^*$  | -0.96 | -0.81 | 0.14  | 0.01 |
| d               | $\text{COH-CHOH-CH}_2\text{OH}^* + * \rightarrow \text{C-CHOH-CH}_2\text{OH}^* + \text{OH}^*$                   | 0.30  | 0.37  | 0.96  | 1.12 |
| d               | $\text{CHOH-COH-CHOH}^* + * \rightarrow \text{CHOH-C-CHOH}^* + \text{OH}^*$                                     | 0.68  | 0.49  | 1.55  | 1.65 |
| d               | $\text{COH-COH-CHOH}^* + * \rightarrow \text{C-COH-CHOH}^* + \text{OH}^*$                                       | 0.40  | 0.20  | 1.05  | 0.94 |
| d               | $\text{COH-CO-CH}_2\text{OH}^* + * \rightarrow \text{C-CO-CH}_2\text{OH}^* + \text{OH}^*$                       | 0.72  | 0.81  | 0.93  | 0.99 |
| d               | $\text{COH-COH-COH}^* + * \rightarrow \text{C-COH-COH}^* + \text{OH}^*$   | 2.53  | 2.07  | 2.92  | 2.43 |
| d               | $\text{CO-COH-CO}^* + * \rightarrow \text{CO-CO-CO}^* + \text{H}^*$   | 0.24  | 0.09  | 0.50  | 0.46 |
| d               | $\text{C-CHOH-CH}_2\text{OH}^* + * \rightarrow \text{C}^* + \text{CHOH-CH}_2\text{OH}^*$                        | -1.23 | 1.04  | -1.02 | 1.18 |
| d               | $\text{C-COH-CHOH}^* + * \rightarrow \text{C}^* + \text{CHOH-COH}^*$  | -0.99 | 0.92  | -1.15 | 0.96 |
| d               | $\text{C-COH-COH}^* + * \rightarrow \text{C}^* + \text{COH-COH}^*$  | -1.12 | 0.90  | -1.35 | 0.95 |
| d               | $\text{CH}_2\text{OH-CO-CH}_2\text{OH}^* + * \rightarrow \text{CH}_2\text{OH}^* + \text{CO-CH}_2\text{OH}^*$    | -1.21 | 1.46  | -1.48 | 1.65 |
| w <sup>43</sup> | $2\text{OH}^* \rightarrow \text{H}_2\text{O}^* + \text{O}^*$  | -0.60 | -0.60 | 0.00  | 0.00 |
| w               | $\text{CO}^* + \text{OH}^* \rightarrow \text{COOH}^* + *$   | -0.20 | -0.20 | 0.51  | 0.51 |
| w               | $\text{COOH}^* + * \rightarrow \text{CO}_2^* + \text{OH}^*$   | -0.44 | -0.44 | 0.00  | 0.00 |
| w               | $\text{COOH}^* + \text{OH}^* \rightarrow \text{CO}_2^* + \text{H}_2\text{O}^*$                                  | 0.40  | 0.40  | 0.97  | 0.97 |
| c <sup>44</sup> | $\text{C}^* + \text{H}^* \rightarrow \text{CH}^* + *$   | -0.58 | -0.58 | 1.25  | 1.25 |
| c               | $\text{CH}^* + \text{H}^* \rightarrow \text{CH}_2^* + *$  | 0.32  | 0.32  | 0.88  | 0.88 |
| c               | $\text{CH}_2^* + \text{H}^* \rightarrow \text{CH}_3^* + *$  | -0.30 | -0.30 | 0.65  | 0.65 |
| c               | $\text{CH}_3^* + \text{H}^* \rightarrow \text{CH}_4^* + *$  | -0.17 | -0.17 | 0.83  | 0.83 |
| e <sup>45</sup> | $\text{CH}^* + \text{C}^* \rightarrow \text{CH-CH}^* + *$   | N/A   | N/A   | 0.90  | 2.04 |
| e               | $\text{CHC}^* + \text{H}^* \rightarrow \text{CH}_2\text{-C}^* + *$  | N/A   | N/A   | 1.10  | 2.22 |
| e               | $\text{CH}_2\text{-C}^* + \text{H}^* \rightarrow \text{CH}_3\text{-C}^* + *$                                    | N/A   | N/A   | 0.99  | 1.33 |
| e               | $\text{CH}_3\text{-C}^* + \text{C}^* \rightarrow \text{CH}_3\text{-C}^* + *$                                    | N/A   | N/A   | 1.04  | 1.95 |
| e               | $2\text{CH}^* \rightarrow \text{CH-CH}^* + *$   | N/A   | N/A   | 1.78  | 2.22 |
| e               | $\text{CH}_2^* + \text{CH}^* \rightarrow \text{CH}_2\text{-CH}^* + *$   | N/A   | N/A   | 1.70  | 1.74 |
| e               | $2\text{CH}_2^* \rightarrow \text{CH}_2\text{-CH}_2^* + *$  | N/A   | N/A   | 1.59  | 2.22 |
| e               | $\text{CH}_3\text{-C}^* + \text{H}^* \rightarrow \text{CH}_3\text{-CH}^* + *$                                   | N/A   | N/A   | 1.13  | 0.28 |
| e               | $\text{CH}_2\text{-C}^* + \text{H}^* \rightarrow \text{CH}_2\text{-CH}^* + *$                                   | N/A   | N/A   | 0.90  | 0.70 |
| e               | $\text{CH}_2\text{-C}^* + \text{H}^* \rightarrow \text{CH}_2\text{-CH}_2^* + *$                                 | N/A   | N/A   | 0.80  | 0.82 |
| e               | $\text{CH}_2\text{-CH}_2^* + \text{H}^* \rightarrow \text{CH}_3\text{-CH}_2^* + *$                              | N/A   | N/A   | 1.27  | 0.63 |
| e               | $\text{CH}_3\text{-CH}_2^* + \text{H}^* \rightarrow \text{CH}_3\text{-CH}_3^* + *$                              | N/A   | N/A   | 0.88  | 0.89 |
| e <sup>42</sup> | $\text{CH}_2\text{OH-CH}_2\text{OH}^* + * \rightarrow \text{CHOH-CH}_2\text{OH}^* + \text{H}^*$                 | -0.40 | -0.38 | 0.83  | 0.72 |
| e               | $\text{CHOH-CH}_2\text{OH}^* + * \rightarrow \text{CHOH-CHOH}^* + \text{H}^*$                                   | -0.45 | -0.42 | 0.36  | 0.33 |
| e               | $\text{CHOH-CH}_2\text{OH}^* + * \rightarrow \text{CHO-CH}_2\text{OH}^* + \text{H}^*$                           | 0.22  | 0.24  | 0.72  | 0.70 |
| e               | $\text{CHOH-CH}_2\text{OH}^* + * \rightarrow \text{CHOH-CH}_2\text{O}^* + \text{H}^*$                           | 0.34  | 0.38  | 0.91  | 0.94 |

|              |   |       |       |      |      |
|--------------|---|-------|-------|------|------|
| e            | $\text{CHOH-CHOH}^* + * \rightarrow 2\text{CHOH}^*$   | -0.09 | 0.02  | 0.98 | 1.00 |
| e            | $\text{CHOH-CHOH}^* + * \rightarrow \text{CHOH-COH}^* + \text{H}^*$   | -0.41 | -0.33 | 0.58 | 0.61 |
| e            | $\text{CHOH-CHOH}^* + * \rightarrow \text{CHOH-CHO}^* + \text{H}^*$   | 0.17  | 0.26  | 0.64 | 0.67 |
| e            | $\text{CHO-CH}_2\text{OH}^* + * \rightarrow \text{CHO}^* + \text{CH}_2\text{OH}^*$  | -0.71 | -0.67 | 1.18 | 1.17 |
| e            | $\text{CHO-CH}_2\text{OH}^* + * \rightarrow \text{CO-CH}_2\text{OH}^* + \text{H}^*$   | -0.89 | -0.85 | 0.20 | 0.30 |
| e            | $\text{CHO-CH}_2\text{OH}^* + * \rightarrow \text{CHOH-CHO}^* + \text{H}^*$   | -0.50 | -0.42 | 0.44 | 0.43 |
| e            | $\text{CO-CH}_2\text{OH}^* + * \rightarrow \text{CO}^* + \text{CH}_2\text{OH}^*$  | -0.91 | -0.85 | 0.61 | 0.67 |
| e            | $\text{CHOH-CH}_2\text{O}^* + * \rightarrow \text{CHOH-CHO}^* + \text{H}^*$   | -0.09 | -0.12 | 0.58 | 0.48 |
| e            | $\text{CHOH-COH}^* + * \rightarrow \text{COH-COH}^* + \text{H}^*$   | -0.32 | -0.30 | 0.69 | 0.64 |
| e            | $\text{CHOH-COH}^* + * \rightarrow \text{COH-CHO}^* + \text{H}^*$   | -0.15 | -0.14 | 0.39 | 0.39 |
| e            | $\text{CHOH-COH}^* + * \rightarrow \text{CHOH-CO}^* + \text{H}^*$   | -0.12 | -0.15 | 0.41 | 0.41 |
| e            | $\text{CHOH-COH}^* + * \rightarrow \text{CHOH}^* + \text{COH}^*$  | -0.24 | -0.26 | 1.03 | 0.99 |
| e            | $\text{CHOH-CHO}^* + * \rightarrow \text{COH-CHO}^* + \text{H}^*$   | -0.43 | -0.38 | 0.31 | 0.33 |
| e            | $\text{CHOH-CHO}^* + * \rightarrow \text{CHOH-CO}^* + \text{H}^*$   | -0.70 | -0.69 | 0.20 | 0.18 |
| e            | $\text{CHOH-CHO}^* + * \rightarrow \text{CHO-CHO}^* + \text{H}^*$   | 0.19  | 0.21  | 0.76 | 0.70 |
| e            | $\text{CHOH-CHO}^* + * \rightarrow \text{CHOH}^* + \text{CHO}^*$  | 0.57  | -0.54 | 0.85 | 0.87 |
| e            | $\text{COH-COH}^* + * \rightarrow \text{COHCO}^* + \text{H}^*$  | -0.33 | -0.29 | 0.47 | 0.47 |
| e            | $\text{COH-CO}^* + * \rightarrow \text{COCO}^* + \text{H}^*$  | -0.11 | -0.06 | 0.43 | 0.43 |
| e            | $\text{CO-CO}^* + * \rightarrow 2\text{CO}^*$   | -1.47 | -1.70 | 0.03 | 0.05 |
| e            | $\text{COH-COH}^* + * \rightarrow 2\text{COH}^*$  | -0.45 | -0.65 | 1.01 | 0.98 |
| e            | $\text{COH-CHO}^* + * \rightarrow \text{CHOCO}^* + \text{H}^*$  | -0.17 | -0.17 | 0.42 | 0.42 |
| e            | $\text{COH-CHO}^* + * \rightarrow \text{COHCO}^* + \text{H}^*$  | -0.78 | -0.79 | 0.26 | 0.29 |
| e            | $\text{COH-CHO}^* + * \rightarrow \text{COH}^* + \text{CHO}^*$  | -0.69 | -0.77 | 0.83 | 0.76 |
| e            | $\text{CHOH-CO}^* + * \rightarrow \text{COHCO}^* + \text{H}^*$  | -0.50 | -0.48 | 0.47 | 0.46 |
| e            | $\text{CHOH-CO}^* + * \rightarrow \text{CHOCO}^* + \text{H}^*$  | 0.10  | 0.14  | 0.59 | 0.60 |
| e            | $\text{CHOH-CO}^* + * \rightarrow \text{CHOH}^* + \text{CO}^*$  | -0.92 | -0.90 | 0.37 | 0.44 |
| e            | $\text{CHO-CHO}^* + * \rightarrow \text{CHOCO}^* + \text{H}^*$  | -0.80 | -0.76 | 0.08 | 0.10 |
| e            | $\text{CHO-CO}^* + * \rightarrow \text{CHO}^* + \text{CO}^*$  | -1.34 | -1.34 | 0.36 | 0.37 |
| e            | $\text{CHO-CHO}^* + * \rightarrow 2\text{CHO}^*$  | -1.08 | -1.07 | 0.75 | 0.75 |
| e            | $\text{CHO}^* + * \rightarrow \text{CO}^* + \text{H}^*$   | -1.04 | -1.03 | 0.20 | 0.23 |
| e            | $\text{COH}^* + * \rightarrow \text{CO}^* + \text{H}^*$   | -0.84 | -0.74 | 0.53 | 0.61 |
| e            | $\text{CHOH}^* + * \rightarrow \text{CHO}^* + \text{H}^*$   | -0.32 | -0.22 | 0.33 | 0.28 |
| e            | $\text{CHOH}^* + * \rightarrow \text{COH}^* + \text{H}^*$   | -0.54 | -0.61 | 0.34 | 0.31 |
| e            | $\text{CH}_2\text{OH}^* + * \rightarrow \text{CHOH}^* + \text{H}^*$   | -0.37 | -0.29 | 0.39 | 0.40 |
| e            | $\text{CH}_3\text{OH}^* + * \rightarrow \text{CH}_2\text{OH}^* + \text{H}^*$  | -0.38 | -0.30 | 0.48 | 0.46 |
| m[This work] | $2\text{H}_2\text{O} + \text{H}^* \rightarrow \text{H}_5\text{O}_2^*$   | N/A   | -0.40 | N/A  | 0.00 |
| m            | $\text{H}_2\text{O} + \text{H}^* \rightarrow \text{H}_3\text{O}^*$  | N/A   | -0.30 | N/A  | 0.00 |
| m            | $\text{CH}_2\text{OH-COH-CH}_2\text{OH}^* + \text{H}_2\text{O}^* \rightarrow \text{CHOH-COH-CH}_2\text{OH}^* + \text{H}_3\text{O}^*$        | N/A   | 0.25  | N/A  | 1.37 |
| m            | $\text{CHOH-COH-CH}_2\text{OH}^* + \text{H}_2\text{O}^* \rightarrow \text{CHOH-COH-CHOH}^* + \text{H}_3\text{O}^*$                          | N/A   | 0.87  | N/A  | 1.61 |
| m            | $\text{CHOH-COH-CHOH}^* + \text{H}_2\text{O}^* \rightarrow \text{CHOH-COH-COH}^* + \text{H}_3\text{O}^*$                                    | N/A   | -0.79 | N/A  | 1.10 |
| m            | $\text{CHOH-COH-COH}^* + \text{H}_2\text{O}^* \rightarrow \text{COH-COH-COH}^* + \text{H}_3\text{O}^*$                                      | N/A   | 0.07  | N/A  | 0.84 |
| m            | $\text{CH}_2\text{OH-COH-CH}_2\text{OH}^* + 2\text{H}_2\text{O}^* \rightarrow \text{CHOH-COH-CH}_2\text{OH}^* + \text{H}_5\text{O}_2^* + *$ | N/A   | 0.25  | N/A  | 1.14 |
| m            | $\text{CHOH-COH-CH}_2\text{OH}^* + 2\text{H}_2\text{O}^* \rightarrow \text{CHOH-COH-CHOH}^* + \text{H}_5\text{O}_2^* + *$                   | N/A   | 0.16  | N/A  | 1.69 |
| m            | $\text{CHOH-COH-CHOH}^* + 2\text{H}_2\text{O}^* \rightarrow \text{CHOH-COH-COH}^* + \text{H}_5\text{O}_2^* + *$                             | N/A   | -1.26 | N/A  | 1.16 |
| m            | $\text{CHOH-COH-COH}^* + 2\text{H}_2\text{O}^* \rightarrow \text{COH-COH-COH}^* + \text{H}_5\text{O}_2 + *$                                 | N/A   | -0.20 | N/A  | 0.55 |

|   |   |     |     |     |      |
|---|---|-----|-----|-----|------|
| m | $\text{COH-COH}^* + \text{H}_2\text{O}^* \rightarrow \text{COH-COH-COH}^* + \text{H}_3\text{O}^*$ | N/A | N/A | N/A | 0.00 |
| m | $\text{COH-CO}^* + \text{H}_2\text{O}^* \rightarrow \text{CO-CO}^* + \text{H}_3\text{O}^*$        | N/A | N/A | N/A | 0.00 |
| m | $\text{CHOH-COH}^* + \text{H}_2\text{O}^* \rightarrow \text{COH-CHO}^* + \text{H}_3\text{O}^*$    | N/A | N/A | N/A | 0.00 |
| m | $\text{CHOH-COH}^* + \text{H}_2\text{O}^* \rightarrow \text{CHOH-CO}^* + \text{H}_3\text{O}^*$    | N/A | N/A | N/A | 0.00 |
| m | $\text{CHOH-CHO}^* + \text{H}_2\text{O}^* \rightarrow \text{CHOH-CO}^* + \text{H}_3\text{O}^*$    | N/A | N/A | N/A | 0.00 |
| m | $\text{CHOH-CHO}^* + \text{H}_2\text{O}^* \rightarrow \text{CHO-CHO}^* + \text{H}_3\text{O}^*$    | N/A | N/A | N/A | 0.00 |
| m | $\text{COH-CHO}^* + \text{H}_2\text{O}^* \rightarrow \text{CHO-CO}^* + \text{H}_3\text{O}^*$      | N/A | N/A | N/A | 0.00 |
| m | $\text{CHOH-CO}^* + \text{H}_2\text{O}^* \rightarrow \text{CHO-CO}^* + \text{H}_3\text{O}^*$      | N/A | N/A | N/A | 0.00 |
| m | $\text{CHO-CHO}^* + \text{H}_2\text{O}^* \rightarrow \text{CHO-CO}^* + \text{H}_3\text{O}^*$      | N/A | N/A | N/A | 0.00 |
| m | $\text{COH}^* + \text{H}_2\text{O}^* \rightarrow \text{CO}^* + \text{H}_3\text{O}^*$              | N/A | N/A | N/A | 0.00 |

## 8 Dominant Reactions and Their Rates from Microkinetic Modeling

The following table lists the dominant reactions of mkm results of reactions under vacuum, at T = 500 K, and initial mole fraction of glycerol = 0.1 in a balance of inerts. The cut-off for a reaction being dominant was set to be 1E-12 mol/s.

Table 9: Dominant reaction steps and corresponding rates at steady state under vacuum.

| Reaction  | Rate (mol site <sup>-1</sup> s <sup>-1</sup> ) |
|---|--|
| $\text{CH}_2\text{OH-CHOH-CH}_2\text{OH} + * \rightarrow \text{CH}_2\text{OH-CHOH-CH}_2\text{OH}^*$               | 7.40E-05                                       |
| $\text{CH}_2\text{OH-CHOH-CH}_2\text{OH}^* + * \rightarrow \text{CH}_2\text{OH-COH-CH}_2\text{OH}^* + \text{H}^*$ | 7.40E-05                                       |
| $\text{CH}_2\text{OH-CHOH-CH}_2\text{OH}^* + * \rightarrow \text{CHOH-CHOH-CH}_2\text{OH}^* + \text{H}^*$         | 1.86E-09                                       |
| $\text{CHOH-CHOH-CH}_2\text{OH}^* + * \rightarrow \text{CHO-CHOH-CH}_2\text{OH}^* + \text{H}^*$                   | 5.52E-06                                       |
| $\text{CHOH-CHOH-CH}_2\text{OH}^* + * \rightarrow \text{CHOH-CHOH-CHOH}^* + \text{H}^*$                           | 8.47E-06                                       |
| $\text{CHOH-CHOH-CHOH}^* + * \rightarrow \text{CHOH-COH-CHOH}^* + \text{H}^*$                                     | 8.47E-06                                       |
| $\text{CHO-CHOH-CH}_2\text{OH}^* + * \rightarrow \text{CO-CHOH-CH}_2\text{OH}^* + \text{H}^*$                     | 5.52E-06                                       |
| $\text{CO-CHOH-CH}_2\text{OH}^* + * \rightarrow \text{CO-CHOH-CHOH}^* + \text{H}^*$                               | 5.52E-06                                       |
| $\text{CO-CHOH-CHOH}^* + * \rightarrow \text{CO}^* + \text{CHOH-CHOH}^*$  | 5.52E-06                                       |
| $\text{CHOH-CHOH}^* + * \rightarrow 2\text{CHOH}^* + *$   | 2.71E-07                                       |
| $\text{CHOH-CHOH}^* + * \rightarrow \text{CHOH-COH}^* + \text{H}^*$   | 1.73E-07                                       |
| $\text{CHOH-CHOH}^* + * \rightarrow \text{CHOH-CHO}^* + \text{H}^*$   | 5.07E-06                                       |
| $\text{CH}_2\text{OH-COH-CH}_2\text{OH}^* + * \rightarrow \text{CHOH-COH-CH}_2\text{OH}^* + \text{H}^*$           | 7.40E-05                                       |
| $\text{CHOH-CHOH-CH}_2\text{OH}^* + * \rightarrow \text{CHOH-COH-CHOH}^* + \text{H}^*$                            | 5.99E-05                                       |
| $\text{CHOH-COH-CH}_2\text{OH}^* + * \rightarrow \text{CHOH-COH-CHOH}^* + \text{H}^*$                             | 6.84E-05                                       |
| $\text{CHOH-CHOH-CHOH}^* + * \rightarrow \text{CHOH-COH-CHOH}^* + \text{H}^*$                                     | 6.84E-05                                       |
| $\text{CHOH-COH-CHOH}^* + * \rightarrow \text{COH-COH-CHOH}^* + \text{H}^*$                                       | 6.84E-05                                       |
| $\text{CHOH-COH-CHOH}^* + * \rightarrow \text{C-COH-CHOH}^* + \text{OH}^*$  | 1.04E-10                                       |
| $\text{OH}^* + \text{CO}^* \rightarrow \text{COOH}^* + *$   | 8.46E-11                                       |
| $\text{OH}^* + \text{H}^* \rightarrow \text{H}_2\text{O}^* + *$   | 5.71E-12                                       |
| $\text{C-COH-CHOH}^* + * \rightarrow \text{COH-CHOH}^* + \text{C}^*$  | 1.04E-10                                       |
| $\text{COH-COH-CHOH}^* + * \rightarrow \text{COH-COH-COH}^* + \text{H}^*$   | 6.84E-05                                       |
| $\text{COH-COH-COH}^* + * \rightarrow \text{CO-COH-COH}^* + \text{H}^*$   | 6.84E-05                                       |
| $\text{CO-COH-COH}^* + * \rightarrow \text{COH-COH}^* + \text{CO}^*$  | 6.84E-05                                       |
| $\text{COHCOH}^* + * \rightarrow \text{COH-CO}^* + \text{H}^*$  | 6.92E-05                                       |
| $\text{COHCO}^* + * \rightarrow \text{CO-CO}^* + \text{H}^*$  | 6.92E-05                                       |
| $\text{COCO}^* + * \rightarrow 2\text{CO}^*$  | 6.92E-05                                       |

|   |          |
|---|----------|
| CO* + CH <sub>2</sub> OH* → CO-CH <sub>2</sub> OH* + *    | 3.83E-10 |
| CO-CH <sub>2</sub> OH* + H* → CHO-CH <sub>2</sub> OH* + * | 3.71E-11 |
| CHOH-COH* + * → COH-CHO* + H*                             | 1.97E-07 |
| CHOH* + H* → CH <sub>2</sub> OH* + *                      | 3.46E-10 |
| CHOH* + * → CHO* + H*                                     | 2.72E-06 |
| CHOH* + * → COH* + H*                                     | 2.19E-06 |
| CHOH-CHO* + * → COH-CHO* + H*                             | 3.07E-07 |
| CHOH-CHO* + * → CHOH-CO* + H*                             | 4.77E-06 |
| CHOH-CHO* + * → CHO-CHO* + H*                             | 6.73E-12 |
| CHOH-CO* + * → COH-CO* + H*                               | 3.58E-07 |
| CHOH-CO* + * → CHO-CO* + H*                               | 1.72E-08 |
| CHOH-CO* + * → CHOH* + CO*                                | 4.37E-06 |
| CHO-CH <sub>2</sub> OH* + * → CH <sub>2</sub> OH* + CHO*  | 3.70E-11 |
| COH-CHO* + * → CHO-CO* + H*                               | 1.97E-08 |
| COH-CHO* + * → COH-CO* + H*                               | 4.84E-07 |
| COH-CHO* + * → COH* + CHO*                                | 1.11E-12 |
| COH-CO* + * → CO* + COH*                                  | 6.92E-05 |
| COH-CO* + * → CO* + COH*                                  | 3.98E-05 |
| CHO* + * → CO* + H*                                       | 2.76E-06 |
| COH* + * → CO* + H*                                       | 2.19E-06 |
| C* + H* → CH* + *   | 3.70E-11 |
| CH* + H* → CH <sub>2</sub> * + *                          | 3.70E-11 |
| CH <sub>2</sub> * + H* → CH <sub>3</sub> * + *            | 3.70E-11 |
| CH <sub>3</sub> * + H* → CH <sub>4</sub> + 2*             | 3.70E-11 |
| CO* → CO + *  | 2.22E-04 |
| 2H* → H <sub>2</sub> + 2*                                 | 2.96E-04 |

The following table lists the dominant reactions of mkm results of reactions in the aqueous phase, at T = 500 K, initial mole fraction of glycerol = 0.1 in a balance of H<sub>2</sub>O. The cut-off for a reaction being dominant was set to be 1E-12 mol/s.

Table 10: Dominant reaction steps and corresponding rates at steady state in the aqueous phase.

| Reaction  | Rate (mol site <sup>-1</sup> s <sup>-1</sup> ) |
|---|--|
| CH <sub>2</sub> OH-CHOH-CH <sub>2</sub> OH + * → CH <sub>2</sub> OH-CHOH-CH <sub>2</sub> OH*      | 1.47E-07                                       |
| CH <sub>2</sub> OH-CHOH-CH <sub>2</sub> OH* + * → CH <sub>2</sub> OH-COH-CH <sub>2</sub> OH* + H* | 1.47E-07                                       |
| CH <sub>2</sub> OH-CHOH-CH <sub>2</sub> OH* + * → CHOH-COH-CH <sub>2</sub> OH* + H*               | 8.55E-11                                       |
| CHOH-CHOH-CH <sub>2</sub> OH* + * → COH-CHOH-CH <sub>2</sub> OH*                                  | 7.05E-12                                       |
| COH-CHOH-CH <sub>2</sub> OH* + * → C-CHOH-CH <sub>2</sub> OH* + OH*                               | 7.05E-12                                       |
| CH <sub>2</sub> OH-COH-CH <sub>2</sub> OH* + * → CHOH-COH-CH <sub>2</sub> OH* + H*                | 1.47E-07                                       |
| CHOH-COH-CH <sub>2</sub> OH* + * → CHOH-COH-CHOH* + H*  | 1.47E-07                                       |
| CHOH-COH-CHOH* + * → COH-COH-CHOH* + H*   | 1.47E-07                                       |
| COH-COH-CHOH* + 2H <sub>2</sub> O → COH-COH-COH* + H <sub>5</sub> O <sub>2</sub> * + *            | 3.27E-08                                       |
| COH-COH-CHOH* + * → COH-COH-COH* + H*   | 1.15E-07                                       |
| COH-COH-CHOH* + H <sub>2</sub> O* → COH-COH-COH* + H <sub>3</sub> O*                              | 7.81E-12                                       |
| COH-COH-CHOH* + 2H <sub>2</sub> O* → COH-COH-COH* + H <sub>5</sub> O <sub>2</sub> * + *           | 3.27E-08                                       |
| COH-COH-COH* + * → COH-COH-CO* + H*   | 1.19E-12                                       |
| COH-COH-COH* + H <sub>2</sub> O* → COH-COH-CO* + H <sub>3</sub> O* + *                            | 4.40E-08                                       |

|   |          |
|---|----------|
| COH-COH-COH* + 2H <sub>2</sub> O* → COH-COH-CO* + H <sub>5</sub> O <sub>2</sub> * + *   | 1.03E-07 |
| COH-COH-CO* + H <sub>2</sub> O* → CO-COH-CO* + H <sub>3</sub> O*                        | 1.00E-08 |
| COH-COH-CO* + * → COH-COH* + CO*  | 1.45E-07 |
| CO-COH-CO* + * → CO-CO-CO* + H*   | 2.09E-09 |
| CO-CO-CO* + * → CO-CO* + CO*  | 2.09E-09 |
| COH-COH* + H <sub>2</sub> O* → COH-CO* + H <sub>3</sub> O*                              | 1.47E-07 |
| COH-CO* + * → CO-CO* + H*   | 1.45E-07 |
| CO-CO* + * → CO* + CO*  | 1.47E-07 |
| 2H* → H <sub>2</sub> + 2*   | 2.39E-07 |
| H <sub>2</sub> O* + * → OH* + H*  | 1.34E-07 |
| H <sub>3</sub> O* + * → H <sub>2</sub> O* + H*  | 7.22E-05 |
| CO* → CO + *  | 1.34E-12 |
| CO* + OH* → COOH* + *   | 1.25E-07 |
| CO* + H <sub>3</sub> O* → COH* + H <sub>2</sub> O*                                      | 6.77E-05 |
| COH* + H* → CHOH* + *   | 2.06E-07 |
| CHOH* + H* → CH <sub>2</sub> OH* + *  | 1.12E-07 |
| COOH* → CO <sub>2</sub> * + H*  | 1.25E-07 |
| CO <sub>2</sub> * → CO <sub>2</sub> + *   | 1.25E-07 |
| CO* + CH <sub>2</sub> OH* → CO-CH <sub>2</sub> OH* + *                                  | 2.11E-09 |
| CO-CH <sub>2</sub> OH* + H* → CHO-CH <sub>2</sub> OH* + *                               | 2.11E-09 |
| CHO-CH <sub>2</sub> OH* + H* → CHOH-CH <sub>2</sub> OH*                                 | 1.19E-05 |
| CHO-CH <sub>2</sub> OH* + * → CHOH-CHO* + H*  | 4.89E-09 |
| CHOH-CH <sub>2</sub> OH* + H* → CH <sub>2</sub> OH-CH <sub>2</sub> OH* + *              | 1.19E-05 |
| CHOH-CHO* + * → CHO-CHO* + H*   | 8.44E-09 |
| CHOH-CHO* + * → CHOH-CO* + H*   | 8.44E-09 |
| CH <sub>2</sub> OH-CH <sub>2</sub> OH* + * → CH <sub>2</sub> O-CH <sub>2</sub> OH* + H* | 1.19E-05 |
| CHO-CHO* + H <sub>2</sub> O* → CHO-CO* + H <sub>3</sub> O*                              | 8.32E-09 |
| CHOH-CO* + H <sub>2</sub> O* → CHO-CO* + H <sub>3</sub> O*                              | 8.61E-09 |
| CH <sub>2</sub> O-CH <sub>2</sub> OH* + * → CHO-CH <sub>2</sub> OH* + H*                | 1.19E-05 |
| CH <sub>2</sub> O-CH <sub>2</sub> OH* + * → CHOH-CH <sub>2</sub> O* + H*                | 1.47E-08 |
| CHO-CH <sub>2</sub> OH* + H* → CHOH-CH <sub>2</sub> OH* + *                             | 1.19E-05 |
| CHO-CH <sub>2</sub> OH* + * → CHOH-CHO* + H*  | 4.89E-09 |
| CHOH-CH <sub>2</sub> O* + * → CHOH-CHO* + H*  | 1.20E-08 |
| CHOH-CH <sub>2</sub> O* + H* → CHOH-CH <sub>2</sub> OH* + *                             | 2.70E-09 |
| CHOH-CH <sub>2</sub> OH* + H* → CH <sub>2</sub> OH-CH <sub>2</sub> OH* + *              | 1.48E-07 |
| CH <sub>2</sub> OH-CH <sub>2</sub> OH* → CH <sub>2</sub> OH-CH <sub>2</sub> OH + *      | 1.58E-07 |

## References

- [1] S. Grimme, *Journal of Computational Chemistry*, 2006, **27**, 1787–1799.
- [2] S. Batsanov, *Inorganic materials*, 2001, **37**, 871–885.
- [3] <https://sites.google.com/a/ncsu.edu/cjobrien/tutorials-and-guides/working-with-water-in-lammps>, (accessed Apr, 2018).
- [4] C. Vega, J. Abascal and I. Nezbeda, *The Journal of Chemical Physics*, 2006, **125**, 034503.

- [5] J. Brodholt and B. Wood, *Journal of Geophysical Research: Solid Earth*, 1993, **98**, 519–536.
- [6] K. Yoshida, C. Wakai, N. Matubayasi and M. Nakahara, *Journal of Chemical Physics*, 2005, **123**, year.
- [7] H. Heinz, T.-J. Lin, R. K. Mishra and F. S. Emami, *Langmuir*, 2013, **29**, 1754–1765.
- [8] W. L. Jorgensen and J. Tirado-Rives, *Journal of the American Chemical Society*, 1988, **110**, 1657–1666.
- [9] J. L. Abascal and C. Vega, *The Journal of Chemical Physics*, 2005, **123**, 234505.
- [10] T. Xie, S. Sarupria and R. B. Getman, *Molecular Simulation*, 2017, **43**, 370–378.
- [11] R. Schimmenti, R. Cortese, L. Godina, A. Prestianni, F. Ferrante, D. Duca and D. Y. Murzin, *The Journal of Physical Chemistry C*, 2017, **121**, 14636–14648.
- [12] J. Zaffran, C. Michel, F. Delbecq and P. Sautet, *Catalysis Science and Technology*, 2016, **6**, 6615–6624.
- [13] Y. Chen, M. Salciccioli and D. G. Vlachos, *The Journal of Physical Chemistry C*, 2011, **115**, 18707–18720.
- [14] B. Liu and J. Greeley, *Physical Chemistry Chemical Physics*, 2013, **15**, 6475.
- [15] C. J. Bodenschatz, S. Sarupria and R. B. Getman, *The Journal of Physical Chemistry C*, 2015, **120**, 801–801.
- [16] J. Nørskov, T. Bligaard, A. Logadottir, S. Bahn, L. Hansen, M. Bollinger, H. Bengaard, B. Hammer, Z. Sljivancanin, M. Mavrikakis, Y. Xu, S. Dahl and C. Jacobsen, *Journal of Catalysis*, 2002, **209**, 275 – 278.
- [17] P. Ferrin, D. Simonetti, S. Kandoi, E. Kunkes, J. A. Dumesic, J. K. Nørskov and M. Mavrikakis, *Journal of the American Chemical Society*, 2009, **131**, 5809–5815.
- [18] B. Liu and J. Greeley, *The Journal of Physical Chemistry C*, 2011, **115**, 19702–19709.
- [19] B. Liu, L. Cheng, L. Curtiss and J. Greeley, *Surface Science*, 2014, **622**, 51–59.
- [20] B. Liu, M. Zhou, M. K. Y. Chan and J. P. Greeley, *ACS Catalysis*, 2015, **5**, 4942–4950.
- [21] R. Alcala, *Journal of Catalysis*, 2003, **218**, 178–190.
- [22] D. Loffreda, F. Delbecq, F. Vigné and P. Sautet, *Angewandte Chemie*, 2009, **121**, 9140–9142.
- [23] G. Henkelman and H. Jónsson, *The Journal of Chemical Physics*, 2000, **113**, 9978–9985.
- [24] G. Henkelman, B. P. Uberuaga and H. Jónsson, *The Journal of Chemical Physics*, 2000, **113**, 9901–9904.
- [25] G. Henkelman and H. Jónsson, *The Journal of Chemical Physics*, 1999, **111**, 7010–7022.
- [26] J. Padró, L. Saiz and E. Guàrdia, *Journal of Molecular Structure*, 1997, **416**, 243–248.
- [27] E. Guàrdia, J. Martí, J. Padró, L. Saiz and A. Komolkin, *Journal of Molecular Liquids*, 2002, **96-97**, 3–17.
- [28] E. Guàrdia, J. Martí, L. García-Tarrés and D. Laria, *Journal of Molecular Liquids*, 2005, **117**, 63–67.
- [29] A. Nag, D. Chakraborty and A. Chandra, *Journal of Chemical Sciences*, 2008, **120**, 71–77.
- [30] T. Xie, <https://github.com/tianjunxie/hbonds>, 2016.
- [31] T. A. Manz and D. S. Sholl, *Journal of Chemical Theory and Computation*, 2010, **6**, 2455–2468.
- [32] T. A. Manz and D. S. Sholl, *Journal of Chemical Theory and Computation*, 2011, **7**, 4146–4164.
- [33] T. A. Manz and D. S. Sholl, *Journal of Chemical Theory and Computation*, 2012, **8**, 2844–2867.

- [34] T. A. Manz and N. G. Limas, *RSC Advances*, 2016, **6**, 47771–47801.
- [35] N. G. Limas and T. A. Manz, *RSC Advances*, 2016, **6**, 45727–45747.
- [36] T. A. Manz, *RSC Adv.*, 2017, **7**, 45552–45581.
- [37] A. P. J. Jansen, in *Modeling Surface Reactions I*, Springer Berlin Heidelberg, Berlin, Heidelberg, 2012, pp. 121–153.
- [38] I. A. Filot, R. J. Broos, J. P. van Rijn, G. J. van Heugten, R. A. van Santen and E. J. Hensen, *ACS Catalysis*, 2015, **5**, 5453–5467.
- [39] I. A. Filot, B. Zijlstra, R. J. Broos, W. Chen, R. Pestman and E. J. Hensen, *Faraday discussions*, 2017, **197**, 153–164.
- [40] M. W. Chase Jr and N.-J. T. Tables, *J. Phys. Chem. Ref. Data, Monograph*, 1998, **9**, 1–1951.
- [41] M. Frisch, G. Trucks, H. B. Schlegel, G. E. Scuseria, M. A. Robb, J. R. Cheeseman, G. Scalmani, V. Barone, B. Mennucci, G. Petersson *et al.*, *Inc., Wallingford, CT*, 2009, **200**, year.
- [42] M. Faheem, M. Saleheen, J. Lu and A. Heyden, *Catalysis Science and Technology*, 2016, **6**, 8242–8256.
- [43] J. P. Clay, J. P. Greeley, F. H. Ribeiro, W. N. Delgass and W. F. Schneider, *Journal of Catalysis*, 2014, **320**, 106–117.
- [44] S. Wang, V. Petzold, V. Tripkovic, J. Kleis, J. G. Howalt, E. Skúlason, E. M. Fernández, B. Hvolbæk, G. Jones, a. Toftelund, H. Falsig, M. Björketun, F. Studt, F. Abild-Pedersen, J. Rossmeisl, J. K. Nørskov and T. Bligaard, *Physical Chemistry Chemical Physics*, 2011, **13**, 20760.
- [45] Y. Chen and D. G. Vlachos, *Journal of Physical Chemistry C*, 2010, **114**, 4973–4982.